

A Grover-compatible Manifold Optimization Algorithm for Quantum Search*

Zhijian Lai¹, Dong An¹, Jiang Hu², and Zaiwen Wen^{†1}

¹Beijing International Center for Mathematical Research, Peking University, Beijing, 100871, People's Republic of China

{lai_zhijian, dongan, wenzw}@pku.edu.cn

²Yau Mathematical Sciences Center, Tsinghua University, Beijing, 100190, People's Republic of China

jianghu@tsinghua.edu.cn

Abstract

Grover's algorithm is a fundamental quantum algorithm that offers a quadratic speedup for the unstructured search problem by alternately applying physically implementable oracle and diffusion operators. In this paper, we reformulate the unstructured search as a maximization problem on the unitary manifold and solve it via the Riemannian gradient ascent (RGA) method. To overcome the difficulty that generic RGA updates do not, in general, correspond to physically implementable quantum operators, we introduce Grover-compatible retractions to restrict RGA updates to valid oracle and diffusion operators. Theoretically, we establish a local Riemannian μ -Polyak-Łojasiewicz (PL) inequality with $\mu = \frac{1}{2}$, which yields a linear convergence rate of $1 - \kappa^{-1}$ toward the global solution. Here, the condition number $\kappa = L_{\text{Rie}}/\mu$, where L_{Rie} denotes the Riemannian Lipschitz constant of the gradient. Taking into account both the geometry of the unitary manifold and the special structure of the cost function, we show that $L_{\text{Rie}} = \mathcal{O}(\sqrt{N})$ for problem size $N = 2^n$. Consequently, the resulting iteration complexity is $\mathcal{O}(\sqrt{N} \log(1/\varepsilon))$ for attaining an ε -accurate solution, which matches the quadratic speedup of $\mathcal{O}(\sqrt{N})$ achieved by Grover's algorithm. These results demonstrate that an optimization-based viewpoint can offer fresh conceptual insights and lead to new advances in the design of quantum algorithms.

1 Introduction

Unstructured search represents a fundamental challenge in computational science, finding broad applications in data retrieval [32, 37], optimization [19, 7, 21], cryptanalysis [23, 10], and machine learning [17, 18]. Its goal is to identify one or more target elements within an unsorted search space of size N . In the absence of exploitable structure, any classical algorithm inevitably requires $\Omega(N)$ queries in the worst case [9], constituting a critical bottleneck for large-scale search tasks.

In 1996, L. K. Grover introduced a groundbreaking quantum algorithm, known as Grover's algorithm [24], which solves the unstructured search problem with a query complexity of $\mathcal{O}(\sqrt{N})$. This quadratic speedup serves as a landmark demonstration of the power of quantum computation over classical algorithms and has become a paradigmatic example of quantum advantage.

*This work was supported by the National Natural Science Foundation of China under the grant numbers 12501419, 12331010 and 12288101, the National Key R&D Program of China under the grant number 2024YFA1012901, the Quantum Science and Technology-National Science and Technology Major Project via Project 2024ZD0301900, and the Fundamental Research Funds for the Central Universities, Peking University.

[†]Corresponding author.

Moreover, this $\mathcal{O}(\sqrt{N})$ query complexity has been rigorously shown to be optimal [41, 53, 9, 8], establishing a tight bound of $\Theta(\sqrt{N})$. The significance of Grover’s algorithm extends far beyond the specific problem of unstructured search. It reveals a fundamental *primitive* of quantum computation. Its underlying mechanism was later generalized to the amplitude amplification (AA) technique [15, 6, 47], an indispensable tool for boosting the success probability of various quantum algorithms [19, 49, 11, 4]. These developments were subsequently unified within the broader framework of quantum singular value transformation (QSVT) [22, 38].

To understand the origin of Grover’s quadratic speedup, several geometric and dynamical interpretations have been proposed. For instance, Grover’s iteration has been characterized as a geodesic in complex projective space connecting the initial and target states [39], and modeled as geodesic dynamics within an information-geometric framework under the Wigner–Yanase metric [16]. More recently, an interpretation based on imaginary-time evolution has been introduced in [48]. Despite these valuable insights, the design of new quantum algorithms still relies largely on specialized constructions and ad hoc reasoning. A unified optimization framework that both explains Grover’s speedups and guides the development of new algorithms has yet to be established.

Manifold (Riemannian) optimization [2, 12, 28] emerges as a compelling framework for understanding Grover’s algorithms. Indeed, manifolds arise naturally in quantum systems, and manifold-based methods have already been successfully applied to tasks such as optimizing quantum circuits [36, 51] and quantum state and comb tomography [27, 34]. In particular, the set of quantum circuits constitutes the unitary manifold $\{U \in \mathbb{C}^{N \times N} \mid U^\dagger U = I\}$. Since many quantum computing tasks aim to find a circuit that prepares a target state or implements a desired transformation, they can be naturally formulated as optimization problems over this unitary manifold [51]. This suggests that manifold optimization can potentially provide a promising and systematic tool for analyzing quantum algorithms.

Recent developments in manifold optimization indicate that algorithm design and convergence theory depend critically on the choice of a *retraction* [5, 2], the operator that maps a tangent vector back onto the manifold and thereby yields the fundamental update step. On the unitary manifold, a natural retraction is the Riemannian exponential¹ map [2, 1], which leads to the update step $U_{k+1} = e^{iHt_k} U_k$. In the context of classical computing, this choice is often replaced by computationally more efficient retractions, such as the Cayley transform [50], QR-based retractions [46, 2], or polar decompositions [3, 2], to avoid explicit matrix exponentials. However, these alternative retractions typically rely on matrix inversions or factorizations that are difficult to realize on quantum hardware, whereas the exponential factor e^{iHt_k} is exactly a quantum gate. Consequently, many retractions that are attractive for a classical computer may not be physically implementable on a quantum computer. Despite the intrinsic suitability of manifold optimization for quantum computing, existing results neither provide an interpretation of Grover-type iterations nor yield Riemannian algorithms with rigorously proven quadratic speedups. This motivates us to develop manifold optimization algorithms whose retractions are compatible with Grover’s quantum gates and to establish convergence guarantees that recover Grover’s quadratic speedup.

1.1 Our contribution

Building on the manifold optimization viewpoint outlined above, our contributions are twofold:

- **Grover-compatible Riemannian gradient ascent algorithms.** We first reformulate the unstructured search problem as a maximization problem on the unitary manifold. We then introduce several *Grover-compatible retractions* on this manifold and employ them to design Riemannian gradient ascent (RGA) algorithms. By construction, each update of

¹The Riemannian exponential map is a geometric concept extending straight lines to manifolds (i.e., geodesics).

these RGA methods is implemented as a finite composition of oracle and diffusion operators. This design ensures that the updates are physically realizable on quantum hardware while simultaneously constituting valid Riemannian retractions within the manifold optimization framework.

- **Linear convergence with Grover’s quadratic speedup.** To analyze the complexity of the our algorithm, we first establish a local Riemannian μ -Polyak–Łojasiewicz (PL) inequality with parameter $\mu = \frac{1}{2}$ for the proposed cost function. This property ensures a linear convergence rate towards the global solution with a per-iteration contraction factor of $1 - \kappa^{-1}$, where the condition number is given by $\kappa = L_{\text{Rie}}/\mu$ and L_{Rie} denotes the Riemannian Lipschitz constant of the gradient. By carefully exploiting the geometry of the unitary manifold and the structure of the cost function, we prove that $L_{\text{Rie}} = \mathcal{O}(\sqrt{N})$ for problem size $N = 2^n$. Consequently, with a step size of order $1/L_{\text{Rie}}$, the resulting Grover-compatible RGA algorithms attain an ε -accurate solution in $\mathcal{O}(\sqrt{N} \log(1/\varepsilon))$ iterations. This result matches Grover’s quadratic speedup in terms of N , while achieving linear convergence with the optimal error dependence $\log(1/\varepsilon)$ under the PL condition.

1.2 Organization

In Section 2, we review the unstructured search problem and the basic geometry of the unitary manifold. In Section 3, we reformulate the search problem as an optimization problem, introduce the Grover-compatible retraction, and derive the associated Riemannian gradient ascent method. We analyze the query complexity in Section 4, showing that our method recovers Grover’s optimal quadratic speedup. Numerical simulations are given in Section 5. We conclude in Section 6.

2 Preliminary

In this section, we begin by reviewing the notation for the unstructured search and introducing the geometric tools required for optimization on the unitary manifold. Afterwards, we summarize the fundamental Riemannian optimization framework that builds upon these ingredients.

2.1 Problem statement

We consider a search problem over the set $[N] = \{0, 1, \dots, N-1\}$, where a binary oracle function $g(x) \in \{0, 1\}$ identifies the marked items. The marked set is denoted as $S = \{x \in [N] : g(x) = 1\}$ with $M := |S|$, and $1 \leq M \ll N$. The task of the search problem is to identify at least one marked item.

The quantum version of the search problem is to prepare a superposition of the marked states. Specifically, let \mathcal{H} be the N -dimensional Hilbert space associated with n qubits and $N = 2^n$, and $\{|j\rangle\}_{j=0}^{N-1}$ denote its computational basis (an orthonormal basis) of \mathcal{H} with the j -th standard basis vector $|j\rangle$. Let the marked subspace be $\mathcal{T} = \text{span}_{\mathbb{C}}\{|x\rangle : x \in S\} \subseteq \mathcal{H}$. Then, the task of the quantum search problem is to prepare a quantum state (i.e., a normalized N -dimensional vector) that lies in \mathcal{T} . The projector onto the marked subspace \mathcal{T} is given by

$$H_g = \sum_{x \in S} |x\rangle\langle x|. \quad (1)$$

Here $\langle x|$ denotes the conjugate transpose of $|x\rangle$. Notice that H_g is Hermitian and idempotent, i.e., $H_g = H_g^\dagger = H_g^2$. The initial state of Grover’s algorithm is the uniform superposition over all computational basis states,

$$|\psi_0\rangle = \frac{1}{\sqrt{N}} \sum_{x=0}^{N-1} |x\rangle, \quad (2)$$

and we denote the corresponding rank-one projector by $\psi_0 = |\psi_0\rangle\langle\psi_0|$. Then, Grover's algorithm is implemented using two types of quantum gates, namely the oracle operator and the diffusion operator, which are defined as follows:

$$U_g(\beta) = e^{i\beta H_g} = I + (e^{i\beta} - 1)H_g, \quad (3)$$

$$D(\alpha) = e^{i\alpha\psi_0} = I + (e^{i\alpha} - 1)\psi_0, \quad (4)$$

where $\alpha, \beta \in \mathbb{R}$ control the rotation angles. Grover's algorithm alternately applies these two operators through $G(\alpha_k, \beta_k) = -D(\alpha_k)U_g(\beta_k)$, so that after T iterations the final state is

$$|\psi_{\text{final}}\rangle = \prod_{k=1}^T G(\alpha_k, \beta_k) |\psi_0\rangle,$$

which is designed to approximate the ideal target state, namely, the uniform superposition over all marked items,

$$|\psi^*\rangle = \frac{1}{\sqrt{M}} \sum_{x \in S} |x\rangle \in \mathcal{T}. \quad (5)$$

The query complexity of the Grover's algorithm is typically considered as the number of calls to $U_g(\beta) = e^{i\beta H_g}$. The circuit implementations of these two types of gates can be found in many standard textbook on quantum computing [31, 41] and are not the focus of this work. In the original formulation of Grover's algorithm [24], the parameters are chosen as $\alpha_k = \beta_k = \pi$ for all k . This choice, however, makes the procedure vulnerable to the soufflé problem [14], where performing too many Grover iterations drives the state past the target instead of toward it when the number of marked states M is underestimated. To solve this overshoot, the so-called $\pi/3$ algorithm [25] prescribes the fixed angles $\alpha_k = \beta_k = \pi/3$, though this modification sacrifices the quadratic speedup. The fixed-point algorithm [52] was introduced to suppress overshooting while still preserving the quadratic speedup.

2.2 Geometric tools on $U(N)$

In the next section, we will reformulate the unstructured search problem above as an optimization problem over the compact Lie group of $N \times N$ unitary matrices:

$$U(N) = \{U \in \mathbb{C}^{N \times N} | U^\dagger U = I_N\}, \quad (6)$$

which is a Riemannian manifold of dimension N^2 . Manifold optimization is deeply rooted in the geometry of manifolds. Here, we present only the minimal set of geometric tools required for our interested manifold $U(N)$. For a systematic treatment of manifold optimization, the reader is referred to textbooks [2, 12].

Tangent space The tangent space at a point on a manifold represents all possible directions in which one can move infinitesimally from that point. For example, on the sphere manifold $\mathbb{S}^{n-1} = \{x \in \mathbb{R}^n : \|x\| = 1\}$, the tangent space at $x \in \mathbb{S}^{n-1}$ is $T_x = \{v \in \mathbb{R}^n : x^T v = 0\} \subseteq \mathbb{R}^n$, which consists of all directions orthogonal to x . Similarly, for the unitary manifold, the tangent space at $U \in U(N)$ is given by

$$T_U = \{\Omega U : \Omega^\dagger = -\Omega\} = \mathfrak{u}(N)U,$$

where $\mathfrak{u}(N) = \{\Omega \in \mathbb{C}^{N \times N} : \Omega^\dagger = -\Omega\}$ denotes the Lie algebra of $U(N)$, i.e., the real vector space of all $N \times N$ skew-Hermitian matrices. Consider the ambient space $\mathbb{C}^{N \times N}$ equipped with the real inner product $\langle A, B \rangle = \Re \text{Tr}(A^\dagger B)$. With respect to this inner product, the orthogonal projection of an arbitrary $Z \in \mathbb{C}^{N \times N}$ onto T_U is given by $\mathcal{P}_U(Z) = \frac{1}{2}(Z - UZ^\dagger U) = \text{Skew}(ZU^\dagger)U \in T_U$ where $\text{Skew}(A) := \frac{1}{2}(A - A^\dagger)$. This construction parallels the projection in the sphere manifold, where $\mathcal{P}_x(z) = z - x(x^T z)$ removes the component of z along x for any $z \in \mathbb{R}^n$.

Riemannian gradient At a point U on the unitary manifold, the Riemannian gradient, $\text{grad } f(U)$, represents the tangent direction of the steepest ascent of a smooth function $f : \mathbb{C}^{N \times N} \rightarrow \mathbb{R}$; it serves as the Riemannian analog of the usual gradient in Euclidean space. Here, we view $\text{U}(N)$ as a Riemannian submanifold of the real vector space $\mathbb{C}^{N \times N} \simeq \mathbb{R}^{2N^2}$. Each tangent space T_U is endowed with the inner product $\langle X, Y \rangle_U := \Re \text{Tr}(X^\dagger Y) = \text{Tr}(\tilde{X}^\dagger \tilde{Y})$, where $X = \tilde{X}U, Y = \tilde{Y}U$, and $\tilde{X}, \tilde{Y} \in \mathfrak{u}(N)$. Under this metric, the Riemannian gradient of f is given by ([12, Proposition 3.61]):

$$\text{grad } f(U) = \mathcal{P}_U(\nabla f(U)) \in T_U, \quad (7)$$

where $\nabla f(U)$ is the usual gradient. Analogously, on the sphere manifold, $\text{grad } f(x) = \nabla f(x) - x(\nabla f(x)^T x)$ for $f : \mathbb{R}^n \rightarrow \mathbb{R}$.

Retractions Retractions provide a mechanism for moving along tangent directions while ensuring that the iterates remain on the manifold. For any $U \in \text{U}(N)$, a retraction is a smooth mapping $R_U : T_U \rightarrow \text{U}(N)$ such that the induced curve $\gamma(t) := R_U(t\eta)$ satisfies

$$\gamma(0) = U \text{ and } \dot{\gamma}(0) = \eta \text{ for all } \eta \in T_U. \quad (8)$$

As a simple example, on the sphere manifold a retraction can be implemented by normalization: $R_x(\eta) = \frac{x+\eta}{\|x+\eta\|}$. A natural case of retraction on $\text{U}(N)$ is Riemannian exponential map, defined by

$$\text{Exp}_U(\eta) = e^{\tilde{\eta}}U, \quad \tilde{\eta} := \eta U^\dagger \in \mathfrak{u}(N). \quad (9)$$

Its induced curve $\gamma(t) = e^{t\tilde{\eta}}U$ satisfies $\gamma(0) = U$ and $\dot{\gamma}(0) = \tilde{\eta}U = \eta$, verifying that Exp_U is a valid retraction. Later, in order to ensure a physically implementable retraction, we will restrict the retraction to a specific subspace of T_U , so that the subsequent Riemannian gradients remain within this subspace.

2.3 Riemannian algorithms

Recall that in the classical setting, to solve $\max_{x \in \mathbb{R}^n} f(x)$, one constructs a sequence $\{x_k\} \subseteq \mathbb{R}^n$ from an initial iterate x_0 via the update rule $x_{k+1} = x_k + t_k \eta_k$, where $\eta_k \in \mathbb{R}^n$ is the search direction and $t_k > 0$ is the step size. The direction η_k can be taken as gradient, or a Newton direction. The step size may be chosen in various ways: as a fixed constant (e.g., reciprocal of the Lipschitz constant), by backtracking to satisfy the Armijo condition [42], by exact line search [42], or by the Barzilai-Borwein rule [44]. Each choice of η_k and t_k gives rise to a different optimization algorithm.

This Euclidean update scheme extends naturally to Riemannian manifolds for solving

$$\max_{U \in \text{U}(N)} f(U), \quad (10)$$

where straight-line updates are replaced by movement along tangent directions, followed by a retraction that maps the iterate back onto the manifold. Given an initial $U_0 \in \text{U}(N)$, the Riemannian update rule constructs a sequence $\{U_k\} \subseteq \text{U}(N)$ via

$$U_{k+1} = R_{U_k}(t_k \eta_k), \quad (11)$$

where $\eta_k \in T_{U_k}$ is the chosen search direction (e.g., Riemannian gradient $\text{grad } f(U_k)$) and $R_{U_k} : T_{U_k} \rightarrow \text{U}(N)$ is a retraction. By choosing appropriate combinations of η_k and t_k , one recovers the Riemannian analogues of classical algorithms, each inheriting the same convergence guarantees as their Euclidean counterparts.

3 Grover-compatible Riemannian algorithm

In this section, we first reformulate the unstructured search problem as a maximization problem over the unitary manifold (as in Eq. (10)) and establish its global optimality conditions. While one could apply standard Riemannian gradient ascent directly, ensuring that each iteration is physically realizable on a quantum device introduces additional challenges. To address this, we introduce the notion of a Grover-compatible retraction, which enables each update to be both physically implementable and fully consistent with the Riemannian optimization framework. Finally, we find that the resulting iteration process is classically simulable, allowing all parameters required to construct the quantum circuit to be precomputed on a classical computer.

3.1 Optimization problem on unitary manifold

We first summarize some properties that can be easily observed in Section 2.1. Applying H_g to the target state yields $H_g |\psi^*\rangle = |\psi^*\rangle$ indicating that $|\psi^*\rangle$ is an eigenstate of H_g associated with eigenvalue 1. Indeed, the spectrum of H_g consists of eigenvalue 1 on the marked subspace \mathcal{T} with multiplicity M , and eigenvalue 0 on its orthogonal complement \mathcal{T}^\perp with multiplicity $N - M$. Let

$$q_0 := \frac{M}{N} \in (0, 1)$$

denote the probability of selecting a marked item uniformly at random. We find that applying H_g to the initial state gives $H_g |\psi_0\rangle = \sqrt{q_0} |\psi^*\rangle$; thus, the initial expectation value satisfies $\langle \psi_0 | H_g | \psi_0 \rangle = \|H_g |\psi_0\rangle\|^2 = \|\sqrt{q_0} |\psi^*\rangle\|^2 = q_0$. Indeed, for any state $|\psi\rangle$, the expectation value $\langle \psi | H_g | \psi \rangle = \sum_{x \in S} |\langle x | \psi \rangle|^2 \in [0, 1]$ represents the probability of observing a marked item when measuring $|\psi\rangle$ in the computational basis. Notice that $\langle \psi^* | H_g | \psi^* \rangle = 1$.

From a high-level view, Grover's algorithm (see Section 2.1) can be interpreted as the process of searching for a quantum state whose expectation value with respect to H_g (thus, the probability of observing a marked item) equals one. To construct such a state, we can adopt the philosophy of quantum circuit design. Starting from an easily prepared state $|\psi_0\rangle$ as the initial state (e.g., Eq. (2)), we aim to design a quantum circuit U whose gates are implementable on quantum hardware (e.g., Eqs. (3) and (4)), such that the resulting state $U |\psi_0\rangle$ becomes an eigenstate of H_g corresponding to its largest eigenvalue 1. Consequently, this leads to the following optimization problem.

Problem 1 (Riemannian optimization formulation). *Let $H = H^\dagger = H^2$ be an orthogonal projector on a Hilbert space \mathcal{H} , and $M := \text{rank}(H)$. Fix a unit vector $|\psi_0\rangle$, and define the rank-one projector $\psi_0 := |\psi_0\rangle\langle\psi_0|$.² Assume that $\langle \psi_0 | H | \psi_0 \rangle \notin \{0, 1\}$. Consider the optimization problem*

$$\max_{U \in \text{U}(N)} f(U), \quad f(U) = \text{Tr} \left(H U \psi_0 U^\dagger \right) = \langle \psi_0 | U^\dagger H U | \psi_0 \rangle, \quad (12)$$

where the feasible region is the compact unitary manifold $\text{U}(N)$ defined in Eq. (6).

We now discuss the connection between the above optimization problem and Grover's algorithm. In Problem 1, the Hermitian observable H is required to satisfy the idempotent condition $H = H^2$, implying that its expectation value $\langle \psi | H | \psi \rangle$ can take values only within the interval $[0, 1]$. The operator H_g introduced in Eq. (1) is a specific instance of such an observable. The initial state $|\psi_0\rangle$ in Problem 1 may be any state satisfying $\langle \psi_0 | H | \psi_0 \rangle \notin \{0, 1\}$; equivalently, $H |\psi_0\rangle \neq 0$ and $H |\psi_0\rangle \neq |\psi_0\rangle$.³ The uniform state $|\psi_0\rangle$ defined in Eq. (2) also constitutes a par-

²In this paper, the kets (e.g., $|\psi\rangle$) denote quantum states, while the corresponding symbols without bra-ket notation (e.g., ψ) represent their associated density operators.

³Since $H = H^\dagger = H^2$, we have $\langle \psi_0 | H | \psi_0 \rangle = \|H |\psi_0\rangle\|^2$. Decompose $|\psi_0\rangle = H |\psi_0\rangle + (I - H) |\psi_0\rangle$ into orthogonal components. Then $1 = \|H |\psi_0\rangle\|^2 + \|(I - H) |\psi_0\rangle\|^2$. Hence, $\langle \psi_0 | H | \psi_0 \rangle = 1$ if and only if $\|(I - H) |\psi_0\rangle\| = 0$, i.e., $H |\psi_0\rangle = |\psi_0\rangle$.

ticular example, as we have shown that $\langle \psi_0 | H_g | \psi_0 \rangle = q_0 \in (0, 1)$. Nevertheless, two differences distinguish the direct optimization formulation in Problem 1 from the Grover's algorithm:

- **Challenge 1.** Grover's algorithm constrains the circuit U to have the specific structure $U = \prod_{k=1}^T G(\alpha_k, \beta_k)$, which arises from physical considerations, as the two types of gates $D(\alpha)$ and $U_g(\beta)$ are easily realizable on quantum hardware. In contrast, Problem 1 imposes no formal restriction on the structure of U .
- **Challenge 2.** Grover's algorithm requires the final output state $U |\psi_0\rangle$ to be the uniform superposition over all marked items, namely the state $|\psi^*\rangle$ defined in Eq. (5). In Problem 1, by comparison, any unit vector within the 1-eigenspace of H constitutes a valid theoretical solution.

In what follows, we will design an optimization algorithm to solve Problem 1 while preserving the two characteristic features of Grover's algorithm discussed above. In this way, we successfully combine Grover's algorithm with optimization techniques, thereby enriching it with new perspectives and strengths drawn from the extensive toolbox and theoretical framework of modern optimization.

3.1.1 Global optimality

For our cost $f(U) = \text{Tr}(HU\psi_0U^\dagger)$ in Problem 1, its Euclidean gradient is $\nabla f(U) = 2HU\psi_0$. Using identity $\text{Skew}(2AB) = [A, B]$ for (skew-)Hermitian matrices A and B , by Eq. (7), we obtain Riemannian gradient:

$$\text{grad } f(U) = \text{Skew}(\nabla f(U)U^\dagger)U = [H, U\psi_0U^\dagger]U \in T_U. \quad (13)$$

Throughout the paper, we use the tilde symbol to denote the skew-Hermitian component associated with an element of $T_U = \mathfrak{u}(N)U$, e.g., $\widetilde{\text{grad } f(U)} = [H, U\psi_0U^\dagger]$. In practice, the rightmost factor U often cancels out, leaving only the skew-Hermitian part as the essential term. Note that $\widetilde{\text{grad } f(U)} = 0$ if and only if $\text{grad } f(U) = 0$.

Let us now examine the optimality conditions of Problem 1 from the perspective of optimization. When the manifold constraint for U is ignored, the cost function f reduces to a standard quadratic function in the Euclidean space $\mathbb{C}^{N \times N} \simeq \mathbb{C}^{N^2}$. In particular, it can be written as

$$f(U) = \text{vec}(U)^\dagger (\psi_0 \otimes H) \text{vec}(U)$$

where $\text{vec}(U) \in \mathbb{C}^{N^2}$ denotes the column-stacked vectorization of matrix U . It is straightforward to verify that $\psi_0 \otimes H$ is positive semidefinite, implying that $f(U)$ is convex in the usual sense. However, once the domain of f is restricted to the compact manifold $\text{U}(N)$, this convexity property is lost, and the problem becomes intrinsically nonconvex. Furthermore, f is not "geodesically convex" (the natural analogue of convexity in manifold sense), because, according to [12, Corollary 11.10], any geodesically convex function defined on a compact manifold must be constant.

Nevertheless, for Problem 1 we can still derive a global optimality condition analogous to the convex case, as stated in Theorem 3.1. In particular, a vanishing Riemannian gradient characterizes global optimality.

Theorem 3.1 (Global optimality). *The skew-Hermitian part of the Riemannian gradient of $f(U)$ in Eq. (12) on $\text{U}(N)$ is given by*

$$\widetilde{\text{grad } f(U)} = [H, \psi_U], \quad \psi_U := U\psi_0U^\dagger,$$

where ψ_U denotes the density operator corresponding to the output state of the circuit U . Then, $\widetilde{\text{grad } f(U^*)} = 0$ if and only if $U^* \in \text{U}(N)$ globally minimizes $f(U)$ over $\text{U}(N)$ with the minimum value 0, or globally maximizes it with the maximum value 1.

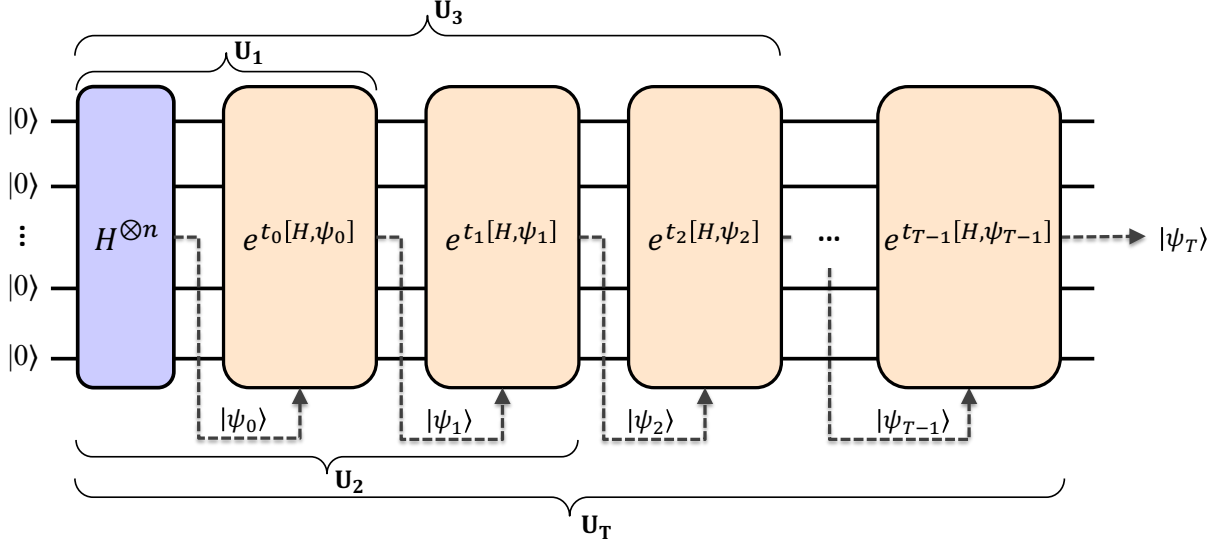


Figure 1: Quantum circuit generated by Riemannian gradient ascent method with the exponential map update Eq. (14), starting from $U_0 = I$ and the uniform state. At each iteration, a new gate $e^{t_k[H, \psi_k]}$ is appended, where $[H, \psi_k]$ is the current Riemannian gradient and t_k is the step size.

Proof. For any Hermitian operator H and any pure state $\psi = |\psi\rangle\langle\psi|$, it holds that $[H, \psi] = 0$ if and only if $H|\psi\rangle = \lambda|\psi\rangle$ for some real λ . Since the eigenvalues of H are $\{0, 1\}$, this condition is equivalent to $H|\psi\rangle = 0$ or $H|\psi\rangle = |\psi\rangle$, i.e., $\langle\psi|H|\psi\rangle \in \{0, 1\}$. \square

3.1.2 Naive Riemannian implementation

Now, if we directly apply update Eq. (11) to Problem 1, we observe that each iteration simply appends new gates to the quantum circuit. We begin by considering the Riemannian gradient ascent (RGA) method with Exponential map $R = \text{Exp}$ in Eq. (9), that takes the update form

$$U_{k+1} = \text{Exp}_{U_k}(t_k \text{grad } f(U_k)) = e^{t_k \widetilde{\text{grad}} f(U_k)} U_k = e^{t_k [H, \psi_k]} U_k, \quad k = 0, 1, \dots, \quad (14)$$

where $\psi_k := U_k \psi_0 U_k^\dagger$ denotes the intermediate quantum state after k -th iterations. Setting the initial gate to $U_0 = I$ and the initial uniform state, the resulting state $|\psi_T\rangle = U_T |\psi_0\rangle$ after T iterations is given by Fig. 1.

The above procedure was also proposed in [51] for general quantum circuit design problems. The overall approach can be summarized as follows: based on the information extracted from the quantum state produced by the current circuit, new gates are added so that the updated circuit output becomes closer to the ground state. This process is then repeated iteratively. Unlike traditional parameterized quantum circuits (PQCs), the ansatz is not fixed but grows dynamically.

Unfortunately, although the above optimization update in Eq. (14) is theoretically valid, we do not know how to efficiently implement the newly added gate $e^{t_k[H, \psi_k]}$ in practice. If we repeatedly pause and perform certain measurements or operations on the current quantum state $|\psi_k\rangle$ to obtain information for approximating $e^{t_k[H, \psi_k]}$, the procedure becomes inefficient as the complexity would grow exponentially in terms of the number of iterations. Therefore, this naive Riemannian implementation is not working. In the following, we propose a more refined approach.

3.2 Grover-compatible retractions

We will introduce the key concept — Grover-compatible retractions, a class of retractions that not only satisfy the standard defining properties in Eq. (8) (albeit restricted to a subspace of the tangent space), thereby ensuring convergence from an optimization standpoint, but also admit a physically implementable structure built from the gates $D(\alpha)$ and $U_g(\beta)$.

3.2.1 Invariant 2D subspace of Riemannian gradients

Throughout the remainder of the paper, let $H = H^\dagger = H^2$ be an orthogonal projector on Hilbert space \mathcal{H} ; let $|\psi_0\rangle \in \mathcal{H}$ be a unit vector and set $\psi_0 = |\psi_0\rangle\langle\psi_0|$. Let $\langle A, B \rangle := \text{Tr}(A^\dagger B)$ denote the Hilbert–Schmidt inner product, and define the Frobenius norm by $\|A\|_F^2 = \langle A, A \rangle$. We begin with an auxiliary lemma.

Lemma 3.2. *Let $\psi = |\psi\rangle\langle\psi|$ be any pure state, and $q := \langle\psi|H|\psi\rangle$. Define the following two skew-Hermitian operators*

$$X := [H, \psi], \quad Y := i[H, X] = i[H, [H, \psi]].$$

Then, it holds that $\|X\|_F = \|Y\|_F = \sqrt{2q(1-q)}$ and $\langle X, Y \rangle = 0$.

Proof. We begin with a useful identity. Since $H^2 = H$, for any matrix A ,

$$[H, [H, [H, A]]] = [H, A]. \quad (15)$$

Applying Eq. (15) with $A = \psi$ gives $[H, [H, X]] = X$. Then,

$$\|Y\|_F^2 = \text{Tr}([H, X]^\dagger [H, X]) = \text{Tr}(X^\dagger [H, [H, X]]) = \text{Tr}(X^\dagger X) = \|X\|_F^2.$$

For the inner product, note that

$$\langle X, Y \rangle = -i \text{Tr}(X[H, X]) = i \text{Tr}(X[X, H]) = i \text{Tr}([X, X]H) = 0.$$

To evaluate $\|X\|_F^2$, we expand $X^\dagger X = \psi H \psi - \psi H \psi H - H \psi H \psi + H \psi H$. Taking the trace and using cyclicity gives

$$\|X\|_F^2 = \text{Tr}(H\psi) + \text{Tr}(H\psi) - 2 \text{Tr}(|\psi\rangle\langle\psi|H|\psi\rangle\langle\psi|H) = 2q(1-q).$$

This completes the proof. \square

The next theorem shows that if the quantum state is evolved using only the two types of gates $D(\alpha)$ and $U_g(\beta)$ appearing in Grover’s algorithm (regardless of how the angle parameters are chosen), then all quantum states remain within the a fixed two-dimensional subspace, namely, *Grover plane* [39], and all skew-Hermitian parts of Riemannian gradients lie in a fixed two-dimensional subspace of the tangent space.

Theorem 3.3 (Invariant 2D gradient subspace). *Initialize the unitary as $U_0 = I$. For $k = 0, 1, \dots$, consider the update rule:*

$$V_k := \text{a finite product of the form } e^{i\theta H} \text{ and } e^{i\theta\psi_0}, \quad U_{k+1} := V_k U_k,$$

and $\psi_k := |\psi_k\rangle\langle\psi_k|$ with $|\psi_k\rangle = U_k|\psi_0\rangle$; i.e., $|\psi_{k+1}\rangle = V_k|\psi_k\rangle$. Define the scalars $q_k := \langle\psi_k|H|\psi_k\rangle \in [0, 1]$, and the skew-Hermitian operators $X_0 := [H, \psi_0]$, $Y_0 := i[H, X_0]$. Then, for all $k \geq 0$:

1. *The state $|\psi_k\rangle$ remains in the fixed 2-dimensional subspace (Grover plane)*

$$|\psi_k\rangle \in \mathcal{S} := \text{span}_{\mathbb{C}}\{|\psi_0\rangle, H|\psi_0\rangle\} \subseteq \mathcal{H}.$$

2. The skew-Hermitian part of Riemannian gradient, $[H, \psi_k]$, remains in the fixed 2-dimensional real subspace

$$[H, \psi_k] \in \mathcal{W} := \text{span}_{\mathbb{R}}\{X_0, Y_0\} \subseteq \mathfrak{u}(N),$$

$$\text{and } \|[H, \psi_k]\|_F = \sqrt{2q_k(1 - q_k)}.$$

Proof. Let

$$|\psi_0\rangle = u + v, \quad u := H|\psi_0\rangle, \quad v := (I - H)|\psi_0\rangle. \quad (16)$$

Since $H^2 = H$ and $(I - H)^2 = I - H$, we have $\|u\|^2 = \langle \psi_0 | H | \psi_0 \rangle = q_0$, $\|v\|^2 = \langle \psi_0 | (I - H) | \psi_0 \rangle = 1 - q_0$, and $u^\dagger v = 0$. Consider the 2-dimensional complex subspace

$$\mathcal{S} := \text{span}_{\mathbb{C}}\{|\psi_0\rangle, H|\psi_0\rangle\} = \text{span}_{\mathbb{C}}\{u, v\}.$$

With the orthogonal decomposition $\mathcal{H} = \mathcal{S} \oplus \mathcal{S}^\perp$, operator identities can be verified by checking their action on each component. Specifically, for any two linear operators $T_1, T_2 : \mathcal{H} \rightarrow \mathcal{H}$, we have $T_1 = T_2 \Leftrightarrow T_1|_{\mathcal{S}} = T_2|_{\mathcal{S}}, T_1|_{\mathcal{S}^\perp} = T_2|_{\mathcal{S}^\perp}$. In our setting, many operators vanish on \mathcal{S}^\perp , so their identities are completely determined by their restrictions to \mathcal{S} .

We first establish the following results regarding the invariance of the subspaces \mathcal{S} and \mathcal{S}^\perp : The operators H, ψ_0 , and their commutator $[H, \psi_0]$ preserve \mathcal{S} , i.e., $H\mathcal{S} \subseteq \mathcal{S}$, $\psi_0\mathcal{S} \subseteq \mathcal{S}$, and therefore $[H, \psi_0]\mathcal{S} \subseteq \mathcal{S}$. Consequently, all operator exponentials of the form $e^{i\theta H}$ and $e^{i\theta \psi_0}$ also preserve \mathcal{S} .⁴ Since each V_k is a finite product of such exponentials, it follows that $V_k\mathcal{S} \subseteq \mathcal{S}$. For (1), we show by induction that all $|\psi_k\rangle$ lie in \mathcal{S} . The base case $|\psi_0\rangle \in \mathcal{S}$ holds by construction. Assuming $|\psi_k\rangle \in \mathcal{S}$, we have $|\psi_{k+1}\rangle = V_k|\psi_k\rangle \in \mathcal{S}$, which completes the induction. On the orthogonal complement \mathcal{S}^\perp , we have $H\mathcal{S}^\perp \subseteq \mathcal{S}^\perp$, $\psi_0\mathcal{S}^\perp = \{0\}$, then $[H, \psi_0]\mathcal{S}^\perp = \{0\}$. Additionally, both $(I - H)\mathcal{S} \subseteq \mathcal{S}$ and $(I - H)\mathcal{S}^\perp \subseteq \mathcal{S}^\perp$ hold. Letting $X_0 = [H, \psi_0]$ and $Y_0 = i[H, X_0]$, we find $Y_0\mathcal{S} \subseteq \mathcal{S}$, and $Y_0\mathcal{S}^\perp = \{0\}$.

To analyze the commutator $[H, \psi_k]$, we select an orthogonal (but non-normalized) basis $\mathcal{B} := \{u, v\}$ of \mathcal{S} . In this basis, the operator H (restricted to \mathcal{S} ; when representing an operator in a basis \mathcal{B} , we implicitly assume that it is restricted to the subspace \mathcal{S}) acts as $Hu = u$ and $Hv = 0$. Therefore,

$$[H]_{\mathcal{B}} = \begin{pmatrix} 1 & 0 \\ 0 & 0 \end{pmatrix}.$$

The rank-one projector $\psi_0 = |\psi_0\rangle\langle\psi_0|$ (with $|\psi_0\rangle = u + v$) acts as $\psi_0 u = q_0(u + v)$ and $\psi_0 v = (1 - q_0)(u + v)$, hence

$$[\psi_0]_{\mathcal{B}} = \begin{pmatrix} q_0 & 1 - q_0 \\ q_0 & 1 - q_0 \end{pmatrix}.$$

It then follows that

$$[X_0]_{\mathcal{B}} = [H, \psi_0]_{\mathcal{B}} = [H]_{\mathcal{B}}[\psi_0]_{\mathcal{B}} - [\psi_0]_{\mathcal{B}}[H]_{\mathcal{B}} = \begin{pmatrix} 0 & 1 - q_0 \\ -q_0 & 0 \end{pmatrix},$$

and, similarly,

$$[Y_0]_{\mathcal{B}} = i[H, X_0]_{\mathcal{B}} = i[H]_{\mathcal{B}}[X_0]_{\mathcal{B}} - i[X_0]_{\mathcal{B}}[H]_{\mathcal{B}} = i \begin{pmatrix} 0 & 1 - q_0 \\ q_0 & 0 \end{pmatrix}.$$

Since $|\psi_k\rangle \in \mathcal{S}$, write it in the unnormalized basis as $|\psi_k\rangle = \alpha_k u + \beta_k v$ for some $\alpha_k, \beta_k \in \mathbb{C}$, (or equivalently $|\psi_k\rangle_{\mathcal{B}} = \begin{pmatrix} \alpha_k \\ \beta_k \end{pmatrix}$) with the normalization condition $\|\psi_k\|^2 = |\alpha_k|^2 q_0 + |\beta_k|^2 (1 - q_0) = 1$. Note that the expectation value of H in state ψ_k is then

$$q_k := \langle \psi_k | H | \psi_k \rangle = (\bar{\alpha}_k u^\dagger + \bar{\beta}_k v^\dagger) H (\alpha_k u + \beta_k v) = |\alpha_k|^2 q_0. \quad (17)$$

⁴If an operator T satisfies $T\mathcal{S} \subseteq \mathcal{S}$, then so does every power T^n , and thus any polynomial $p(T)$ or convergent power series $f(T) = \sum c_n T^n$ maps \mathcal{S} into itself. In particular, this holds for $e^{i\theta H}$ and $e^{i\theta \psi_0}$.

A direct calculation yields

$$[\psi_k]_{\mathcal{B}} = \begin{pmatrix} |\alpha_k|^2 q_0 & \alpha_k \bar{\beta}_k (1 - q_0) \\ \bar{\alpha}_k \beta_k q_0 & |\beta_k|^2 (1 - q_0) \end{pmatrix} = \begin{pmatrix} q_k & (1 - q_0) z_k \\ q_0 \bar{z}_k & 1 - q_k \end{pmatrix},$$

where we define $z_k := \alpha_k \bar{\beta}_k$. We compute

$$[H, \psi_k]_{\mathcal{B}} = [H]_{\mathcal{B}} [\psi_k]_{\mathcal{B}} - [\psi_k]_{\mathcal{B}} [H]_{\mathcal{B}} = \begin{pmatrix} 0 & (1 - q_0) z_k \\ -q_0 \bar{z}_k & 0 \end{pmatrix}.$$

This can be decomposed as

$$[H, \psi_k]_{\mathcal{B}} = \Re z_k [X_0]_{\mathcal{B}} + \Im z_k [Y_0]_{\mathcal{B}}. \quad (18)$$

Thus, we have verified the equality relations of the three operators restricted to \mathcal{S} . Note that for $|\psi_k\rangle = (*)H|\psi_0\rangle + (*)(I - H)|\psi_0\rangle$, we have $\psi_k = (*)H\psi_0H + (*)(I - H)\psi_0H + (*)H\psi_0(I - H) + (*)(I - H)\psi_0(I - H)$, where $(*)$ denotes constants. From the above expression, we obtain that $\psi_k \mathcal{S} \subseteq \mathcal{S}$ and $\psi_k \mathcal{S}^\perp = \{0\}$. It then follows that $[H, \psi_k] \mathcal{S} \subseteq \mathcal{S}$ and $[H, \psi_k] \mathcal{S}^\perp = \{0\}$. Finally, noting that $X_0 \mathcal{S}^\perp = Y_0 \mathcal{S}^\perp = \{0\}$, we conclude that, on the entire Hilbert space \mathcal{H} ,

$$[H, \psi_k] = \Re z_k X_0 + \Im z_k Y_0 \in \text{span}_{\mathbb{R}} \{X_0, Y_0\} = \mathcal{W}.$$

This completes the proof that $[H, \psi_k] \in \mathcal{W}$ for all $k \geq 0$. For norm $\|[H, \psi_k]\|_F = \sqrt{2q_k(1 - q_k)}$, see Lemma 3.2. \square

3.2.2 Grover-compatible retractions

In what follows, whenever it causes no ambiguity, the term *gradient* will also refer to the skew-Hermitian component of the Riemannian gradient. Likewise, when discussing the subspace $\mathcal{W}U \subseteq \mathfrak{u}(N)U = T_U$, we sometimes, for simplicity, focus on $\mathcal{W} \subseteq \mathfrak{u}(N)$ itself and disregard the right U . Recall the notations

$$X_0 := [H, \psi_0], \quad Y_0 := i[H, X_0], \quad \mathcal{W} := \text{span}_{\mathbb{R}} \{X_0, Y_0\} \subseteq \mathfrak{u}(N).$$

Our key idea is to restrict the optimization dynamics to the fixed 2D subspace \mathcal{W} . At the initial step $k = 0$, the gradient $[H, \psi_0]$ belongs to \mathcal{W} . So we assume that, at some iteration k , the current gradient $[H, \psi_k]$ lies in \mathcal{W} . Next, we may employ an elaborate retraction, termed the Grover-compatible retraction R_U below, to update.

Definition 3.4 (Grover-compatible retraction). For all $U \in U(N)$:

1. $R_U : \mathcal{W}U \rightarrow U(N)$ is a well-defined retraction on $\mathcal{W}U \subseteq T_U$, namely, for all $\eta \in \mathcal{W}U$, the induced curve $\gamma(t) = R_U(t\eta)$ for $t \geq 0$, satisfies $\gamma(0) = U$ and $\dot{\gamma}(0) = \eta$ for all $\eta \in \mathcal{W}U$.
2. R_U has the form $R_U = \underbrace{(\text{a finite product of the form } e^{i\theta H} \text{ and } e^{i\theta\psi_0})}_{\text{newly added gates } V :=} \times U$.

Remark 3.1. Since the step sizes in our algorithms are always positive, we may safely restrict the domain of the curve $\gamma(t)$ to $t \geq 0$. This modification has no impact on the subsequent theoretical analysis but helps avoid certain technical subtleties. In this setting, $\dot{\gamma}(0)$ should be understood as the right-hand derivative.

Given a Grover-compatible retraction R_U , we naturally choose the tangent direction η_k to be the current gradient. Then, the update $U_{k+1} = R_{U_k}(t_k \eta_k)$ is well-defined, since the current gradient $\tilde{\eta}_k = [H, \psi_k]$ lies within \mathcal{W} . By construction, the additional circuit components V introduced by R_U consist solely of gates of the form $e^{i\theta H}$ and $e^{i\theta\psi_0}$. According to Theorem 3.3,

such an update preserves the subspace invariance property, ensuring that the next gradient $[H, \psi_{k+1}]$ also remains in \mathcal{W} .

Repeating this process iteratively, the Riemannian gradient ascent (RGA) method based on the Grover-compatible R_U exactly follows the iterative structure described in Theorem 3.3, ensuring that each gradient $[H, \psi_k]$ always stays within \mathcal{W} . Finally, since the mapping R_U satisfies the axioms of a valid retraction (the term 2 in Definition 3.4; though restricted to \mathcal{W}), the standard convergence guarantees of Riemannian optimization remain applicable.

Indeed, there exist numerous retractions that fulfill Definition 3.4, with varying structures and lengths. Three representative examples are given next proposition. It is worth noting that while we label them as 8-factor, 6-factor, and 5-factor retractions, there are multiple possible realizations for each given length.

Proposition 3.5. *For all $U \in \mathcal{U}(N)$ and any $\eta \in \mathcal{W}U$, decompose the skew-Hermitian part $\tilde{\eta} := \eta U^\dagger \in \mathcal{W}$ as $\tilde{\eta} = xX_0 + yY_0$ for unique coefficients $(x, y) \in \mathbb{R}^2$. The following are some Grover-compatible retractions as in Definition 3.4.*

- **8-factor retraction.** Define

$$R_U^{(8)}(\eta) := e^{i\frac{y}{2}\psi_0} e^{i\frac{\pi}{2}H} e^{-i\frac{x}{2}\psi_0} e^{-i\pi H} e^{i\frac{x}{2}\psi_0} e^{-i\frac{\pi}{2}H} e^{-i\frac{y}{2}\psi_0} e^{i\pi H} U.$$

We can show that $\gamma(t) = R_U^{(8)}(t\eta)$ satisfies $\gamma(0) = U$ and $\dot{\gamma}(0) = \eta \in \mathcal{W}U$.

- **6-factor retraction.** Define

$$R_U^{(6)}(\eta) := e^{i\frac{\pi}{2}H} e^{ic_1\psi_0} e^{-i\pi H} e^{ic_2\psi_0} e^{i\frac{\pi}{2}H} e^{iyt\psi_0} U,$$

where $c_1 := -\frac{x+y}{2}$, and $c_2 := \frac{x-y}{2}$. We can show that $\gamma(t) = R_U^{(6)}(t\eta)$ satisfies $\gamma(0) = U$ and $\dot{\gamma}(0) = \eta \in \mathcal{W}U$.

- **5-factor retraction.** Let $A := \text{atan2}(y, x)$, $R := \sqrt{x^2 + y^2}$, (the argument and modulus of the complex number $x + iy$) and set

$$a_1 = A + \frac{\pi}{2}, \quad a_2 = A - \frac{\pi}{2}, \quad b_1 = -\frac{R}{2}, \quad b_2 = \frac{R}{2}. \quad (19)$$

Define

$$R_U^{(5)}(\eta) := e^{ia_1H} e^{ib_1\psi_0} e^{i(a_2-a_1)H} e^{ib_2\psi_0} e^{-ia_2H} U. \quad (20)$$

Since $a_2 - a_1 = -\pi$, the middle H -factor simplifies to $e^{-i\pi H}$. Then,

$$\gamma(t) = R_U^{(5)}(t\eta) = \underbrace{e^{ia_1H} e^{itb_1\psi_0} e^{i(a_2-a_1)H} e^{itb_2\psi_0} e^{-ia_2H}}_{\text{newly added gates } V(t):=} U, \quad t \geq 0. \quad (21)$$

We can show that $\gamma(t)$ satisfies $\gamma(0) = U$ and $\dot{\gamma}(0) = \eta \in \mathcal{W}U$.

Proof. We provide the proof only for the 5-factor retraction, as the arguments for the other cases are similar. Let ad_H be the linear map on matrices, $\text{ad}_H(A) := [H, A]$. The identity $[H, [H, [H, A]]] = [H, A]$ in Eq. (15) implies $\text{ad}_H^3 = \text{ad}_H$. Then, any power of ad_H reduces to one of the three operators I, ad_H , or ad_H^2 . In fact, by applying the adjoint action identity in [26, Proposition 3.35] (the second equality below), we obtain

$$\Psi(\theta) := e^{i\theta H} \psi_0 e^{-i\theta H} = \sum_{n \geq 0} \frac{(i\theta)^n}{n!} \text{ad}_H^n(\psi_0) = \psi_0 + i \sin \theta X_0 + (\cos \theta - 1) [H, [H, \psi_0]].$$

Since $Y_0 := i[H, X_0] = i[H, [H, \psi_0]]$, we have $[H, [H, \psi_0]] = -iY_0$. Hence

$$i\Psi(\theta) = i\psi_0 - \sin \theta X_0 + (\cos \theta - 1)Y_0. \quad (22)$$

For any $U \in \text{U}(N)$ and $\eta \in \mathcal{W}U$, write the skew-Hermitian part $\tilde{\eta} := \eta U^\dagger \in \mathcal{W}$ as $\tilde{\eta} = xX_0 + yY_0$. Consider the induced curve $\gamma(t)$ in Eq. (21) with parameters are given in Eq. (19). At $t = 0$, $\gamma(0) = e^{ia_1 H} e^{i(a_2 - a_1)H} e^{-ia_2 H} U = e^{i0 \cdot H} U = U$. Only the ψ_0 -exponentials depend on t , so by the product rule,

$$\begin{aligned} \dot{V}(0) &= ib_1 e^{ia_1 H} \psi_0 e^{-i(\pi + a_2)H} + ib_2 e^{i(a_1 - \pi)H} \psi_0 e^{-ia_2 H} \\ &= ib_1 \underbrace{e^{ia_1 H} \psi_0 e^{-ia_1 H}}_{\Psi(a_1) :=} + ib_2 \underbrace{e^{ia_2 H} \psi_0 e^{-ia_2 H}}_{\Psi(a_2) :=}, \end{aligned}$$

where we used $a_1 - \pi = a_2$ and $\pi + a_2 = a_1$. Therefore

$$\begin{aligned} \dot{V}(0) &= ib_1 \Psi(a_1) + ib_2 \Psi(a_2) \\ &= i(b_1 + b_2) \psi_0 - (b_1 \sin a_1 + b_2 \sin a_2) X_0 + (b_1 (\cos a_1 - 1) + b_2 (\cos a_2 - 1)) Y_0. \end{aligned}$$

With $b_1 = -R/2$ and $b_2 = R/2$, we have $b_1 + b_2 = 0$, so the $i\psi_0$ term vanishes. Using $a_1 = A + \frac{\pi}{2}$, $a_2 = A - \frac{\pi}{2}$, then $\sin a_1 = \cos A$, $\sin a_2 = -\cos A$, $\cos a_1 = -\sin A$, $\cos a_2 = \sin A$. Hence, $-(b_1 \sin a_1 + b_2 \sin a_2) = R \cos A$, and $b_1 (\cos a_1 - 1) + b_2 (\cos a_2 - 1) = R \sin A$. Therefore, $\dot{V}(0) = (R \cos A) X_0 + (R \sin A) Y_0 = xX_0 + yY_0 = \tilde{\eta}$. Finally, $\dot{\gamma}(0) = \dot{V}(0)U = \tilde{\eta}U = \eta$. This completes the proof. \square

Indeed, Grover-compatible retractions $R_U : \mathcal{W}U \simeq \mathbb{R}^2 \rightarrow \text{U}(N)$ admit the following general form:

$$R_U(\eta) = \underbrace{\left(\prod_{\ell=1}^K e^{i\theta_\ell^{(1)}(t;x,y)H} e^{i\theta_\ell^{(2)}(t;x,y)\psi_0} \right)}_{V(t;x,y) :=} U, \quad (23)$$

for some finite integer K , and $\tilde{\eta} = xX_0 + yY_0$. (The order of H - and ψ_0 -exponentials in the expressions above does not matter.)

3.2.3 Grover-compatible Riemannian gradient ascent method

Now, we provide the Riemannian gradient ascent (RGA) method employing Grover-compatible retractions in Algorithm 1. Moreover, the resulting state $|\psi_T\rangle = U_T|\psi_0\rangle$ after T iterations (KT calls to $e^{i\theta H}$) is given by Fig. 2.

Algorithm 1 Riemannian gradient ascent method using the Grover-compatible retraction (RGA-Grover)

- 1: Choose a Grover-compatible retraction R in Definition 3.4 with formula Eq. (23), initial point U_0 , and tolerance ε . Set $q_0 := \text{Tr}(H\psi_0)$.
- 2: Set $k := 0$.
- 3: **while** $\|\text{grad } f(U_k)\| > \varepsilon$ **do**
- 4: Decompose $\text{grad } f(U_k) = [H, \psi_k] = x_k X_0 + y_k Y_0$ to find $(x_k, y_k) \in \mathbb{R}^2$.
- 5: Choose a step size $t_k > 0$.
- 6: Update by Eq. (23),

$$U_{k+1} = R_{U_k}(t_k \text{ grad } f(U_k)) = V(t_k; x_k, y_k) U_k. \quad (24)$$

- 7: Update the state $|\psi_{k+1}\rangle := V(t_k; x_k, y_k)|\psi_k\rangle$.
 - 8: Compute new cost value $q_{k+1} := \langle \psi_{k+1} | H | \psi_{k+1} \rangle$.
 - 9: Compute norm $\|\text{grad } f(U_{k+1})\|_F = \sqrt{2q_{k+1}(1 - q_{k+1})}$.
 - 10: Set $k := k + 1$.
 - 11: **end while**
-

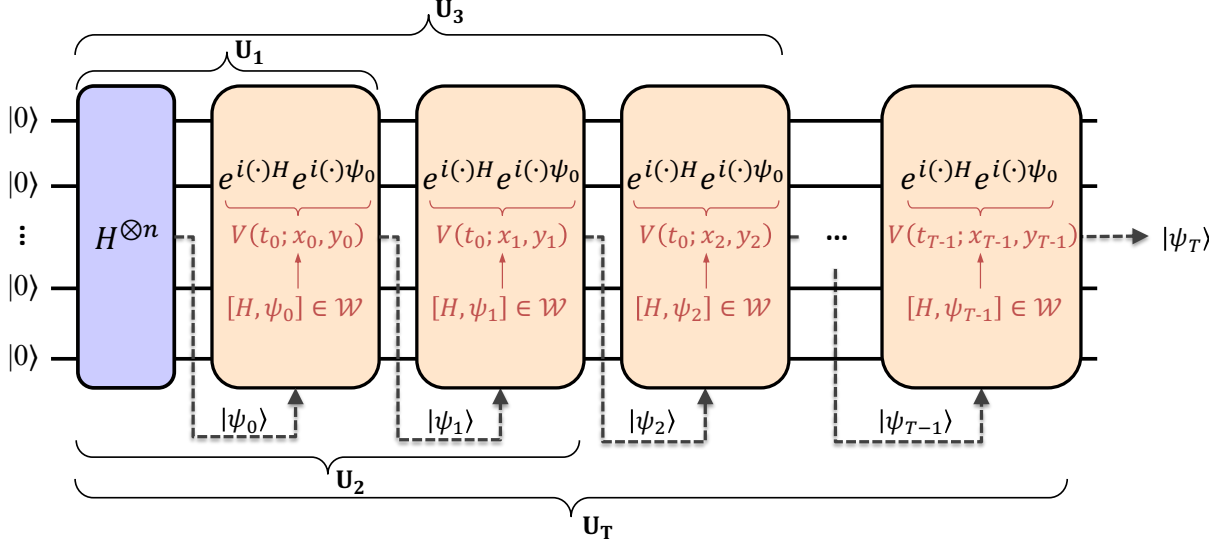


Figure 2: Quantum circuit generated by Riemannian gradient ascent method with the Grover-compatible retraction update Eq. (24), starting from $U_0 = I$ and the uniform state. At each iteration, a new gate $V(t_k; x_k, y_k)$ is appended.

This procedure is essentially identical to the standard Riemannian optimization algorithm, yet it preserves the defining feature of Grover’s algorithm: every circuit consists solely of gates of the form $e^{i\theta H}$ and $e^{i\theta\psi_0}$. The key difference is that we now use gradient information to adaptively choose the rotation angle θ . At this point, Challenge 1 in Section 3.1 has been resolved. For Challenge 2, we make the following simple observation. Let $q_0 := \langle \psi_0 | H | \psi_0 \rangle$ and define the target state $|\psi^*\rangle := (1/\sqrt{q_0})H | \psi_0 \rangle$. For any $|\psi_k\rangle \in \mathcal{S} = \text{span}_{\mathbb{C}}\{|\psi_0\rangle, H|\psi_0\rangle\}$, the cost value $q_k := \langle \psi_k | H | \psi_k \rangle = |\langle \psi_k | \psi^* \rangle|^2$. Thus, when $q_k \rightarrow 1$, the states $|\psi_k\rangle$ and $|\psi^*\rangle$ differ only by a global phase and are therefore physically indistinguishable. In the Grover setting, with $H = H_g$ and $|\psi_0\rangle$ defined in Eqs. (1) and (2), the state $|\psi^*\rangle := (1/\sqrt{q_0})H | \psi_0 \rangle$ exactly matches the ideal target state in Eq. (5). Hence, starting from the uniform superposition over all items, the algorithm necessarily converges to the uniform superposition over all marked items.

3.3 Classical simulability of Algorithm 1

A main concern is how to compute the gradient coordinates (x_k, y_k) in Algorithm 1. We know that x_k (likewise for y_k) can be obtained via the inner product $x_k = \langle [H, \psi_k], X_0 \rangle / (2q_0(1 - q_0))$, which seems to suggest that one might need to perform certain measurements on the current quantum state $|\psi_k\rangle$ before proceeding with the circuit update. In fact, this is not an issue.

The following theorem shows that all key quantities generated throughout Algorithm 1 at each iteration, including the cost values q_k , the gradient coordinates (x_k, y_k) within \mathcal{W} , are classically simulatable. That is, the entire iterative process of Algorithm 1 can be fully simulated on a classical computer. Once all angles have been computed, this Grover-type circuit can then be implemented accordingly.

Theorem 3.6 (2D reduced dynamics). *Consider the iterative process and notation introduced in Algorithm 1. With initialization triplet $(x_0, y_0, q_0) := (1, 0, q_0)$, define the 2×2 matrix $\Psi_0 = \begin{pmatrix} q_0 & 1 - q_0 \\ q_0 & 1 - q_0 \end{pmatrix}$. Then there exists an explicit, classically computable process*

$$F : (x_k, y_k, q_k; t_k) \mapsto (x_{k+1}, y_{k+1}, q_{k+1}) \quad (25)$$

described as follows. For each $k = 0, 1, \dots$,

1. If $k = 0$, set $\alpha_k = 1$, $\beta_k = 1$ and $z_k = \alpha_k \bar{\beta}_k$. ($\alpha_k, \beta_k, z_k \in \mathbb{C}$ are auxiliary variables)
2. For the additional gate sequence in update Eq. (24):

$$V(t_k; x_k, y_k) = \prod_{\ell=1}^K e^{i\theta_\ell^{(1)}(t_k; x_k, y_k) H} e^{i\theta_\ell^{(2)}(t_k; x_k, y_k) \psi_0},$$

define the corresponding 2×2 matrix

$$M_k := M(t_k; x_k, y_k) = \prod_{\ell=1}^K E_H(\theta_\ell^{(1)}(t_k; x_k, y_k)) E_{\psi_0}(\theta_\ell^{(2)}(t_k; x_k, y_k)), \quad (26)$$

where $E_H(\theta) = \begin{pmatrix} e^{i\theta} & 0 \\ 0 & 1 \end{pmatrix}$ and $E_{\psi_0}(\theta) = I_2 + (e^{i\theta} - 1)\Psi_0$.

3. Update

$$\begin{aligned} \begin{bmatrix} \alpha_{k+1} \\ \beta_{k+1} \end{bmatrix} &\leftarrow M_k \begin{bmatrix} \alpha_k \\ \beta_k \end{bmatrix}, \text{ and} \\ q_{k+1} &\leftarrow q_0 |\alpha_{k+1}|^2, \quad z_{k+1} \leftarrow \alpha_{k+1} \bar{\beta}_{k+1}, \quad x_{k+1} \leftarrow \Re z_{k+1}, \quad y_{k+1} \leftarrow \Im z_{k+1}. \end{aligned}$$

Proof. We follow all notations introduced in the proof of Theorem 3.3. Let $\mathcal{B} = \{u, v\}$ denote the orthogonal (but non-normalized) basis of the Grover plane \mathcal{S} , defined in Eq. (16). By Theorem 3.3, for all k , the states $|\psi_k\rangle$ lie in \mathcal{S} . Hence, we can write

$$|\psi_k\rangle = \alpha_k u + \beta_k v, \quad \alpha_k, \beta_k \in \mathbb{C},$$

or equivalently, $|\psi_k\rangle_{\mathcal{B}} = \begin{pmatrix} \alpha_k \\ \beta_k \end{pmatrix} \in \mathbb{C}^2$. We further define $z_k := \alpha_k \bar{\beta}_k$ for all $k = 0, 1, \dots$, as in the proof of Theorem 3.3. For $k = 0$, since $|\psi_0\rangle = u + v$, we have $\alpha_0 = 1$, $\beta_0 = 1$, and therefore $z_0 = 1$. Since $|\psi_{k+1}\rangle = V(t_k; x_k, y_k)|\psi_k\rangle$, it follows that

$$|\psi_{k+1}\rangle_{\mathcal{B}} = M_k |\psi_k\rangle_{\mathcal{B}}, \quad \text{i.e.,} \quad \begin{bmatrix} \alpha_{k+1} \\ \beta_{k+1} \end{bmatrix} = M_k \begin{bmatrix} \alpha_k \\ \beta_k \end{bmatrix},$$

where M_k denotes the matrix representation of the operator $V(t_k; x_k, y_k)$. By Eqs. (17) and (18), we have $q_{k+1} = q_0 |\alpha_{k+1}|^2$, $x_{k+1} = \Re(z_{k+1})$, and $y_{k+1} = \Im(z_{k+1})$. It remains to derive the explicit form of M_k . We have already shown that

$$[H]_{\mathcal{B}} = \begin{pmatrix} 1 & 0 \\ 0 & 0 \end{pmatrix}, \quad \Psi_0 := [\psi_0]_{\mathcal{B}} = \begin{pmatrix} q_0 & 1 - q_0 \\ q_0 & 1 - q_0 \end{pmatrix}.$$

Using the projector identity $e^{i\theta P} = I + (e^{i\theta} - 1)P$ for any $P^2 = P$, we define the following 2×2 matrices:

$$E_H(\theta) = I_2 + (e^{i\theta} - 1)[H]_{\mathcal{B}} = \begin{pmatrix} e^{i\theta} & 0 \\ 0 & 1 \end{pmatrix}, \quad E_{\psi_0}(\theta) = I_2 + (e^{i\theta} - 1)\Psi_0.$$

Hence, the matrix representation of the operator $V(t_k; x_k, y_k)$ is given by Eq. (26), which depends on the step size t_k and the gradient coordinates x_k, y_k . \square

4 Complexity analysis

It is well known that Grover's algorithm achieves a query complexity of $\mathcal{O}(\sqrt{N/M})$, yielding a quadratic speedup over classical search. Moreover, any quantum algorithm for the unstructured search problem must use at least $\Omega(\sqrt{N/M})$ queries [53], establishing that the $\mathcal{O}(\sqrt{N/M})$ bound is optimal. Since the previous section showed how Grover's algorithm integrates cleanly into a Riemannian optimization framework, a natural question arises: *Can standard complexity analysis techniques from optimization theory also recover the $\mathcal{O}(\sqrt{N/M})$ result?*

In this section, we recover the optimal scaling using tools from Riemannian optimization. We begin by carefully estimating the Riemannian Lipschitz constant L_{Rie} and show that $L_{\text{Rie}} = \mathcal{O}(\sqrt{N/M})$. Next, a local Riemannian μ -Polyak-Łojasiewicz (PL) inequality with $\mu = \frac{1}{2}$ is established. Combining these two regularity conditions yields an iteration complexity of $\mathcal{O}(\sqrt{N/M} \log(1/\varepsilon))$ for Algorithm 1 to reach an ε -global maximizer, in agreement with Grover's quadratic speedup.

4.1 Riemannian Lipschitz constants

When optimizing a cost function in Euclidean space, its (gradient) Lipschitz constant is a crucial quantity in the analysis of iteration complexity. Similarly, for optimizations defined on a manifold, one can also introduce notions of Riemannian Lipschitz continuity/constants intrinsic to the manifold. In this subsection, we will compute the Riemannian Lipschitz constant of our cost function on the unitary manifold. We begin with the following lemma, which provides its Lipschitz constant in the Euclidean setting.

Lemma 4.1 (Euclidean Lipschitz constant). *Consider the cost function $f(U) = \text{Tr}(HU\psi_0U^\dagger)$, then the Euclidean gradient $\nabla f(U) = 2HU\psi_0$ is Lipschitz continuous with (smallest) constant $L_{\text{Euc}} = 2$, i.e.,*

$$\|\nabla f(U_1) - \nabla f(U_2)\|_F \leq 2\|U_1 - U_2\|_F, \quad \text{for all } U_1, U_2 \in \mathbb{C}^{N \times N}.$$

Proof. Since H and ψ_0 are projectors, their spectral norms $\|H\|_2 = \|\psi_0\|_2 = 1$. For any $U_1, U_2 \in \mathbb{C}^{N \times N}$,

$$2\|H(U_1 - U_2)\psi_0\|_F \leq 2\|H\|_2\|\psi_0\|_2\|U_1 - U_2\|_F = 2\|U_1 - U_2\|_F.$$

Thus the smallest Lipschitz constant $L_{\text{Euc}} \leq 2$. We next show that it is tight. Let $w = |\psi_0\rangle$ so that $\psi_0 = ww^\dagger$, and choose a unit vector $v \in \text{range}(H) = \{v \in \mathbb{C}^N : Hv = v\}$ (since $H^2 = H$). Set $A := vw^\dagger$. Then $\|A\|_F = \|v\|\|w\| = 1$, and $\|HA\psi_0\|_F = \|Hvw^\dagger ww^\dagger\|_F = \|(Hv)w^\dagger\|_F = \|Hv\|\|w\| = \|v\| = 1$. Choose U_1, U_2 such that $U_1 - U_2 = A$, then $\|\nabla f(U_1) - \nabla f(U_2)\|_F = 2\|HA\psi_0\|_F = 2\|A\|_F$. Hence, $L_{\text{Euc}} = 2$. \square

Recall that notations $X_0 := [H, \psi_0]$, $Y_0 := i[H, X_0]$, and $\mathcal{W} := \text{span}_{\mathbb{R}}\{X_0, Y_0\} \subseteq \mathfrak{u}(N)$. By Lemma 3.2, we have

$$c_0 := \|X_0\|_F = \|Y_0\|_F = \|[X_0, \psi_0]\|_F = \frac{\sqrt{2M(N-M)}}{N}, \quad (27)$$

since $c_0 = \sqrt{2q_0(1-q_0)}$ and $q_0 = \text{Tr}(H\psi_0) = \frac{M}{N}$. Next, we establish two important bounds for Grover-compatible retractions. For concreteness, we present the proof using the 5-factor retraction as an example; the arguments for other retractions proceed in an analogous manner.

Lemma 4.2 (Tight first and second order bounds). *Consider the 5-factor retraction $R_U \equiv R_U^{(5)}$ defined in Eq. (20). For all $U \in \text{U}(N)$ and $\eta \in \mathcal{W}U$, we have*

$$\|R_U(\eta) - U\|_F \leq \|\eta\|_F, \quad \|R_U(\eta) - U - \eta\|_F \leq \frac{1}{4c_0}\|\eta\|_F^2.$$

Moreover, both are globally tight: $\frac{\|R_U(\eta) - U\|_F}{\|\eta\|_F} \rightarrow 1$, $\frac{\|R_U(\eta) - U - \eta\|_F}{\|\eta\|_F^2} \rightarrow \frac{1}{4c_0}$, as $\eta \rightarrow 0$.

Proof. Because X_0 and Y_0 are orthogonal under the Frobenius inner product and both have norm $\|X_0\|_F = \|Y_0\|_F = c_0$, we obtain

$$\|\eta\|_F = \|\tilde{\eta}\|_F = c_0 \sqrt{x^2 + y^2} = c_0 R.$$

We first establish the first-order bound. Consider the induced curve

$$\gamma(t) := R_U(t\eta) = e^{ia_1 H} e^{itb_1 \psi_0} (e^{-i\pi H}) e^{itb_2 \psi_0} e^{-ia_2 H} U, \quad t \in [0, 1]. \quad (28)$$

Notice that the middle term can be written as $e^{-i\pi H} = I + (e^{-i\pi} - 1)H = I - 2H$. Differentiating $\gamma(t)$ with respect to t only through the ψ_0 -exponentials gives

$$\begin{aligned} \gamma'(t) &= e^{ia_1 H} e^{itb_1 \psi_0} \left(\frac{iR}{2} [e^{-i\pi H}, \psi_0] \right) e^{itb_2 \psi_0} e^{-ia_2 H} U \\ &= e^{ia_1 H} e^{itb_1 \psi_0} \underbrace{(-iRX_0)}_{M:=} e^{itb_2 \psi_0} e^{-ia_2 H} U, \end{aligned} \quad (29)$$

where we used $[e^{-i\pi H}, \psi_0] = [I - 2H, \psi_0] = -2[H, \psi_0] = -2X_0$. Left and right multiplication by unitaries preserve the Frobenius norm, so $\|\gamma'(t)\|_F = R \|X_0\|_F = \|\eta\|_F$, $\forall t \in [0, 1]$. Using the integral form of the first-order Taylor expansion, $\gamma(1) = \gamma(0) + \int_0^1 \gamma'(t) dt$, we obtain

$$\|R_U(\eta) - U\|_F = \left\| \int_0^1 \gamma'(t) dt \right\|_F \leq \int_0^1 \|\gamma'(t)\|_F dt = \|\eta\|_F.$$

Because $\gamma'(0) = \eta$, it follows that $\|R_U(\eta) - U\|_F = \|\eta\|_F + o(\|\eta\|_F)$ ($\eta \rightarrow 0$). Thus, the constant 1 in the bound is globally tight.

We now establish the second-order bound. Differentiating $\gamma'(t)$ in Eq. (29) once more, treating M as $e^{-i\pi H}$ in Eq. (28), yields

$$\begin{aligned} \gamma''(t) &= e^{ia_1 H} e^{itb_1 \psi_0} \left(\frac{iR}{2} [M, \psi_0] \right) e^{itb_2 \psi_0} e^{-ia_2 H} U \\ &= e^{ia_1 H} e^{itb_1 \psi_0} \left(\frac{R^2}{2} [X_0, \psi_0] \right) e^{itb_2 \psi_0} e^{-ia_2 H} U. \end{aligned}$$

Therefore, $\|\gamma''(t)\|_F = \frac{R^2}{2} \|X_0, \psi_0\|_F = \frac{R^2}{2} c_0$, $\forall t \in [0, 1]$. Using the integral form of the second-order Taylor expansion, $\gamma(1) = \gamma(0) + \gamma'(0) + \int_0^1 (1-t) \gamma''(t) dt$, we have

$$\begin{aligned} \|R_U(\eta) - U - \eta\|_F &= \left\| \int_0^1 (1-t) \gamma''(t) dt \right\|_F \\ &\leq \int_0^1 (1-t) \|\gamma''(t)\|_F dt = \frac{1}{2} \cdot \frac{R^2}{2} c_0 = \frac{1}{4c_0} \|\eta\|_F^2. \end{aligned}$$

Moreover, since $R_U(\eta) = U + \eta + \frac{1}{2} \gamma''(0) + o(\|\eta\|_F^2)$, and $\|\gamma''(0)\|_F = \frac{R^2}{2} c_0$, it follows that $\frac{\|R_U(\eta) - U - \eta\|_F}{\|\eta\|_F^2} = \frac{1}{4c_0} + o(1)$ ($\eta \rightarrow 0$), which establishes that the constant $1/(4c_0)$. We complete the proofs. \square

We are now ready to compute the Riemannian Lipschitz constant of f . Due to the intricacy of Riemannian geometry, extending Lipschitz continuity/constants to manifolds can be cumbersome, and several definitions appear in the literature. Here, we follow the approach recommended in [13], which uses a pullback descent inequality. This method avoids additional geometric machinery and allows the analysis to be carried out entirely with Euclidean tools while still supporting the convergence results that follow. The next Proposition 4.3 establishes the Riemannian Lipschitz constant of the cost in Problem 1 on the unitary manifold. Notably, such constant L_{Rie} scales as $\sqrt{N/M}$, increasing with the problem size $N = 2^n$.

Proposition 4.3 (Riemannian Lipschitz constant). *Consider the 5-factor retraction $R_U \equiv R_U^{(5)}$ defined in Eq. (20). Let*

$$L_{\text{Rie}} := 2 + \frac{N}{\sqrt{2M(N-M)}} \in \mathcal{O}\left(\sqrt{\frac{N}{M}}\right). \quad (30)$$

Then, for all $U \in \mathcal{U}(N)$, the pullbacks $f \circ R_U : \mathcal{W}U \rightarrow \mathbb{R}$ satisfy

$$|f(R_U(\eta)) - [f(U) + \langle \text{grad } f(U), \eta \rangle]| \leq \frac{L_{\text{Rie}}}{2} \|\eta\|_F^2, \quad \forall \eta \in \mathcal{W}U.$$

Proof. By Lemma 4.1, the Euclidean gradient $\nabla f(U)$ is Lipschitz continuous over the entire Euclidean space $\mathbb{C}^{N \times N}$ with constant $L_{\text{Euc}} = 2$. Hence, by the well-known descent lemma (see, e.g., [40, Lemma 1.2.3]), for all $U, W \in \mathcal{U}(N) \subseteq \mathbb{C}^{N \times N}$,

$$|f(W) - [f(U) + \langle \nabla f(U), W - U \rangle]| \leq \frac{L_{\text{Euc}}}{2} \|W - U\|_F^2 = \|W - U\|_F^2.$$

In particular, this inequality holds for $W := R_U(\eta)$ with $\eta \in \mathcal{W}U$. Let $\Delta := R_U(\eta) - U \in \mathbb{C}^{N \times N}$, then

$$|f(R_U(\eta)) - [f(U) + \langle \nabla f(U), \Delta \rangle]| \leq \|\Delta\|_F^2. \quad (31)$$

Since the Riemannian gradient $\text{grad } f(U)$ is the orthogonal projection of $\nabla f(U)$ onto T_U , see Eq. (7), we have

$$\langle \nabla f(U), \Delta \rangle = \langle \nabla f(U), \eta + (\Delta - \eta) \rangle = \langle \text{grad } f(U), \eta \rangle + \langle \nabla f(U), \Delta - \eta \rangle. \quad (32)$$

Substituting (32) into (31) yields

$$\underbrace{|f(R_U(\eta)) - [f(U) + \langle \text{grad } f(U), \eta \rangle]|}_{A:=} - \underbrace{\langle \nabla f(U), \Delta - \eta \rangle}_{B:=} \leq \|\Delta\|_F^2.$$

Then, we have $|A| \leq |A - B| + |B| \leq \|\Delta\|_F^2 + |\langle \nabla f(U), \Delta - \eta \rangle|$. By the Cauchy–Schwarz inequality and Lemma 4.2, we obtain

$$\begin{aligned} |A| &\leq \|R_U(\eta) - U\|_F^2 + \|\nabla f(U)\|_F \|R_U(\eta) - U - \eta\|_F \\ &\leq \|\eta\|_F^2 + \frac{2}{4c_0} \|\eta\|_F^2 = (1 + \frac{1}{2c_0}) \|\eta\|_F^2, \end{aligned}$$

where we used the fact $\|\nabla f(U)\|_F = \|2HU\psi_0\|_F \leq 2\|H\|_2 \|U\|_2 \|\psi_0\|_F = 2$. Setting $L_{\text{Rie}} := 2(1 + \frac{1}{2c_0}) = 2 + \frac{1}{c_0}$ and combining this with Eq. (27) complete the proof. \square

4.2 Complexity results

Using Proposition 4.3 and extending the standard nonconvex complexity technique to the manifold setting [13], we obtain the following baseline complexity.

Theorem 4.4 (Baseline Complexity). *Consider Problem 1 in the Grover setting, where the initial success probability is $q_0 = f(U_0) = M/N$. Suppose we run Algorithm 1 with the 5-factor retraction $R_U \equiv R_U^{(5)}$ defined in Eq. (20), and choose a fixed step size $t_k = 1/L_{\text{Rie}}$, where $L_{\text{Rie}} = \mathcal{O}(\sqrt{N/M})$ is given in Eq. (30). Then, for any $\varepsilon > 0$,*

$$T \geq \left\lceil \frac{2L_{\text{Rie}}}{\varepsilon^2} \right\rceil \implies \min_{0 \leq k \leq T-1} \|\text{grad } f(U_k)\| \leq \varepsilon.$$

Proof. This theorem is a direct application of [13, Corollary 2.9]. \square

For a fixed accuracy ε , the above result recovers the well-known $\mathcal{O}(\sqrt{N/M})$ complexity of Grover's algorithm by noting $L_{\text{Rie}} = \mathcal{O}(\sqrt{N/M})$. We will now show that the dependence on ε can be improved from $1/\varepsilon^2$ to $\log(1/\varepsilon)$. This refinement relies on establishing an explicit Riemannian PL condition for Problem 1, as shown below.

Proposition 4.5 (PL condition of Problem 1). *The Riemannian PL inequality holds locally for problem (12), namely, for any $U \in \mathcal{U}(N)$ such that $f(U) \geq \frac{1}{2}$,*

$$\|\text{grad } f(U)\|^2 \geq 1 - f(U). \quad (33)$$

Proof. It follows from Lemma 3.2 that $\|\text{grad } f(U)\|^2 = 2f(U)(1 - f(U))$. Applying $f(U) \geq \frac{1}{2}$ yields the desired result. \square

The μ -PL inequality Eq. (33), first introduced in [43, 35], has become a central tool for establishing global linear convergence of $1 - \kappa^{-1}$ with $\kappa = L/\mu$ (where L could be L_{Euc} or L_{Rie}) for gradient-type methods [30, 45] beyond the strongly convex setting. In the theorem below, we use it to obtain the global linear convergence of RGA.

Theorem 4.6 (Best Complexity). *Consider the same assumptions as in Theorem 4.4. Let $q_k := f(U_k) \in [0, 1]$. Then, for any $0 < \varepsilon \leq q_0$, the iterates satisfy $1 - q_T \leq \varepsilon$ in at most*

$$T = \left\lceil 6L_{\text{Rie}} \log \left(\frac{1}{\varepsilon} \right) \right\rceil.$$

Proof. Let $\delta_k := 1 - q_k$. For each iterate U_k , by Lemma 3.2 (or term 2 of Theorem 3.3), we have $\|\text{grad } f(U_k)\|^2 = 2q_k(1 - q_k)$. By Proposition 4.3, for each k , the pullbacks $f \circ R_{U_k} : \mathcal{W}U_k \rightarrow \mathbb{R}$ satisfy

$$\begin{aligned} f(U_{k+1}) &= f(R_{U_k}(\eta_k)) \geq f(U_k) + \langle \text{grad } f(U_k), \eta_k \rangle - \frac{L_{\text{Rie}}}{2} \|\eta_k\|^2 \\ &\geq f(U_k) + (t_k - \frac{L_{\text{Rie}}}{2} t_k^2) \|\text{grad } f(U_k)\|^2 \\ &= f(U_k) + \frac{1}{2L_{\text{Rie}}} \|\text{grad } f(U_k)\|^2, \end{aligned} \quad (34)$$

where we used $\eta_k = t_k \text{grad } f(U_k)$ together with the step size choice $t_k = 1/L_{\text{Rie}}$ from Algorithm 1. In terms of $q_k = f(U_k)$, Eq. (34) can be written as

$$q_{k+1} \geq q_k + \frac{1}{2L_{\text{Rie}}} \cdot 2q_k(1 - q_k) = q_k + \frac{q_k(1 - q_k)}{L_{\text{Rie}}}. \quad (35)$$

In particular, the sequence $\{q_k\}_{k \geq 0}$ is nondecreasing.

Phase I: From $q_0 = M/N$ to $q_k \geq \frac{1}{2}$. Whenever $q_k \leq \frac{1}{2}$, we have $1 - q_k \geq \frac{1}{2}$, and thus Eq. (35) implies

$$q_{k+1} \geq q_k + \frac{q_k}{2L_{\text{Rie}}} = q_k \left(1 + \frac{1}{2L_{\text{Rie}}} \right). \quad (36)$$

Let $K := \min \{k \geq 0 : q_k \geq \frac{1}{2}\}$ be the first index at which the sequence reaches the level $\frac{1}{2}$. We construct an explicit upper bound for K . Define

$$K_0 := \left\lceil \frac{\log \left(\frac{1}{2q_0} \right)}{\log \left(1 + \frac{1}{2L_{\text{Rie}}} \right)} \right\rceil \leq \frac{\log \left(\frac{1}{2q_0} \right)}{\log \left(1 + \frac{1}{2L_{\text{Rie}}} \right)} + 1.$$

We now verify that $K \leq K_0$. If some $k < K_0$ already satisfies $q_k \geq \frac{1}{2}$, then by definition $K \leq k < K_0$. Otherwise, if $q_j < \frac{1}{2}$ holds for all $j < K_0$, then Eq. (36) applies to every such j , and induction yields

$$q_{K_0} \geq q_0 \left(1 + \frac{1}{2L_{\text{Rie}}} \right)^{K_0} \geq q_0 \cdot \frac{1}{2q_0} = \frac{1}{2},$$

which again implies $K \leq K_0$.

Using the inequality $\log(1+x) \geq x/2$ for $0 < x \leq 1$, and substituting $x := 1/(2L_{\text{Rie}}) \leq 1/4$, we obtain $\log\left(1 + \frac{1}{2L_{\text{Rie}}}\right) \geq \frac{1}{4L_{\text{Rie}}} \Rightarrow \frac{1}{\log\left(1 + \frac{1}{2L_{\text{Rie}}}\right)} \leq 4L_{\text{Rie}}$. Hence,

$$K \leq K_0 \leq 4L_{\text{Rie}} \cdot \log\left(\frac{1}{2q_0}\right) + 1. \quad (37)$$

Therefore, the sequence $\{q_k\}$ reaches the level $q_k \geq \frac{1}{2}$ in at most $4L_{\text{Rie}} \log(1/(2q_0)) + 1$ iterations. This completes the analysis of Phase I.

Phase II: Linear convergence by the PL property in the region $q_k \geq \frac{1}{2}$. From Phase I, we have that for all $k \geq K$, $q_k = f(U_k) \geq \frac{1}{2}$. Using Eq. (34) and the PL inequality Eq. (33), it holds

$$\delta_{k+1} = 1 - f(U_{k+1}) \leq 1 - f(U_k) - \frac{1}{2L_{\text{Rie}}} \|\text{grad } f(U_k)\|^2 \leq \left(1 - \frac{1}{2L_{\text{Rie}}}\right) \delta_k$$

for all $k \geq K$. By induction, this yields

$$\delta_k \leq \delta_K \left(1 - \frac{1}{2L_{\text{Rie}}}\right)^{k-K} \leq \left(1 - \frac{1}{2L_{\text{Rie}}}\right)^{k-K}, \quad \forall k \geq K.$$

To hope $\delta_T \leq \varepsilon$ for some iteration $T \geq K$, it is sufficient to require $\left(1 - \frac{1}{2L_{\text{Rie}}}\right)^{T-K} \leq \varepsilon$. Taking logarithms on both sides yields $(T - K) \log\left(1 - \frac{1}{2L_{\text{Rie}}}\right) \leq \log(\varepsilon)$, i.e.,

$$T - K \geq \frac{\log(\varepsilon)}{\log\left(1 - \frac{1}{2L_{\text{Rie}}}\right)} = \frac{\log\left(\frac{1}{\varepsilon}\right)}{-\log\left(1 - \frac{1}{2L_{\text{Rie}}}\right)}, \quad (38)$$

since $\log\left(1 - \frac{1}{2L_{\text{Rie}}}\right) < 0$. Since $\log(1-x) \leq -x$ for all $0 < x < 1$, we have $\frac{1}{-\log(1-x)} \leq \frac{1}{x}$. Substituting $x := 1/(2L_{\text{Rie}}) \leq 1/4$, we obtain $2L_{\text{Rie}} \geq \frac{1}{-\log\left(1 - \frac{1}{2L_{\text{Rie}}}\right)}$. Thus a sufficient condition for Eq. (38) is

$$T - K \geq 2L_{\text{Rie}} \cdot \log\left(\frac{1}{\varepsilon}\right). \quad (39)$$

In other words, if we choose $T \geq K + 2L_{\text{Rie}} \log\left(\frac{1}{\varepsilon}\right)$, then $\delta_T \leq \varepsilon$.

Phase III: A unified complexity result. Combining the bounds Eqs. (37) and (39) obtained in Phases I and II, we obtain the unified sufficient condition

$$T \geq 4L_{\text{Rie}} \log\left(\frac{1}{2q_0}\right) + 1 + 2L_{\text{Rie}} \log\left(\frac{1}{\varepsilon}\right). \quad (40)$$

We now show that the simpler requirement

$$T \geq 6L_{\text{Rie}} \log\left(\frac{1}{\varepsilon}\right) \quad (41)$$

implies Eq. (40) under the assumption $0 < \varepsilon \leq q_0$. Since $\frac{2q_0}{\varepsilon} \geq 2$ and $L_{\text{Rie}} \geq 2$, we have

$$4L_{\text{Rie}} \log\left(\frac{1}{\varepsilon}\right) - 4L_{\text{Rie}} \log\left(\frac{1}{2q_0}\right) = 4L_{\text{Rie}} \log\left(\frac{2q_0}{\varepsilon}\right) \geq 4L_{\text{Rie}} \log 2 \geq 8 \log 2 > 1.$$

Consequently, $4L_{\text{Rie}} \log\left(\frac{1}{\varepsilon}\right) + 2L_{\text{Rie}} \log\left(\frac{1}{\varepsilon}\right) \geq \left(4L_{\text{Rie}} \log\frac{1}{2q_0} + 1\right) + 2L_{\text{Rie}} \log\left(\frac{1}{\varepsilon}\right)$. Therefore, whenever the condition Eq. (41) holds, the more detailed sufficient condition Eq. (40) is automatically satisfied. Hence, under Eq. (41), we indeed have $\delta_T \leq \varepsilon$. \square

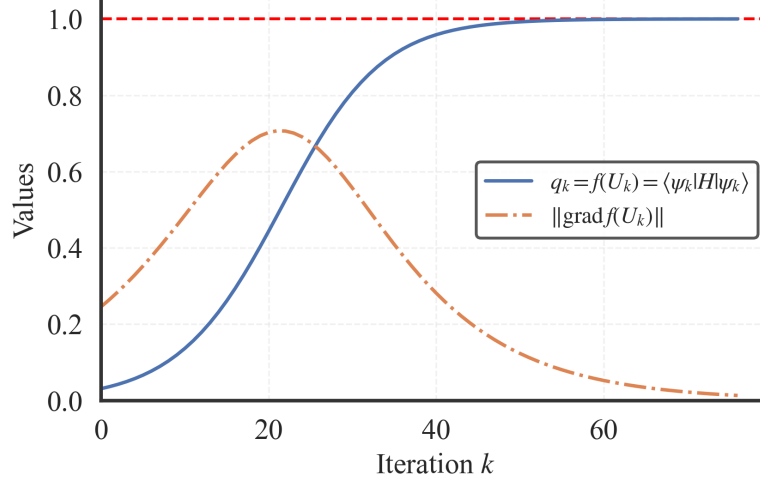


Figure 3: Representative optimization trajectory for $n = 6$ qubits using the 5-factor retraction with fixed step size $t_k = 1/L_{\text{Rie}}$. The cost value q_k increases smoothly toward its maximal value 1, illustrating the characteristic behavior of a typical gradient ascent method.

Regarding complexity, researchers in quantum computing and those in optimization focus on different aspects. Optimization researchers typically fix the problem size N and study how the number of iterations T depends on the target accuracy ε . In contrast, quantum computing researchers usually fix the accuracy ε and investigate how the iteration count scales with the problem size N , namely, the qubits n . It is worth noting that the obtained complexity $\mathcal{O}(\sqrt{N/M} \log(1/\varepsilon))$ not only shows that the Grover-compatible Riemannian gradient ascent achieves a linear convergence rate for this nonconvex problem, but also matches the optimal $\sqrt{N/M}$ scaling of Grover’s algorithm.

5 Numerical simulations

In this section, we validate the theoretical findings using numerical simulations. Because Algorithm 1 is classically simulatable due to Theorem 3.6, all experiments are implemented directly using NumPy. All simulations were performed on a MacBook Pro (2021) with an Apple M1 Pro processor, 16 GB RAM. The source code is publicly available.⁵

Let $N = 2^n$ for an n -qubit system, and unless otherwise noted we always take size of marked items $M = 1$. The progress of the algorithm is measured by the cost value $q_k = f(U_k) = \text{Tr}(H\psi_k)$ which corresponds to the success probability of identifying the marked item. Given an accuracy $\varepsilon > 0$, the algorithm terminates once $|1 - q_k| < \varepsilon$.

Representative optimization trajectory We begin by illustrating a typical optimization process. Set $n = 6$ and $\varepsilon = 10^{-4}$, we apply the 5-factor Grover-compatible retraction with a fixed step size $t_k = 1/L_{\text{Rie}}$; see Eq. (30). Fig. 3 reports the evolution of the cost value q_k , and the norm of the Riemannian gradient $\|\text{grad } f(U_k)\| = \|[H, \psi_k]\|$. The curve of q_k exhibits the smooth and monotone improvement characteristic of typical gradient ascent methods.

Scaling with problem size Next, we investigate how the iteration complexity scales with the problem size N . We fix $\varepsilon = 10^{-4}$ and vary the number of qubits from $n = 2$ to $n = 25$, so that \sqrt{N} ranges from 2 to $\sqrt{2^{25}} \approx 5792$. In Algorithm 1, we consider two strategies for step sizes. The first is the fixed $t_k = 1/L_{\text{Rie}}$, applied together with the 5-factor retraction. The second is

⁵https://github.com/GALVINLAI/RGA_Grover

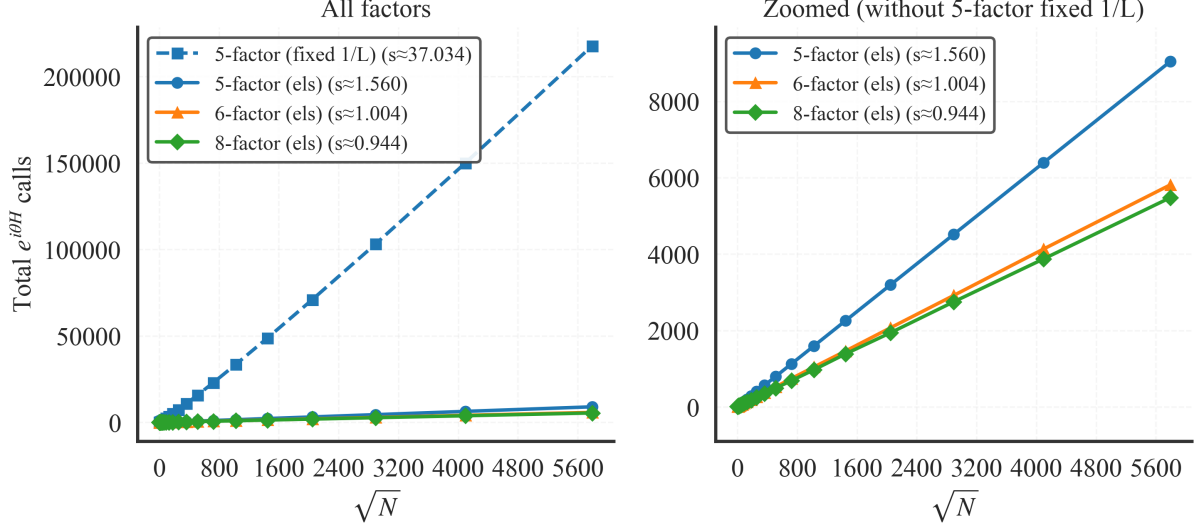


Figure 4: Scaling of the total number of H -exp calls with problem size \sqrt{N} for different Grover-compatible retractions and step size strategies. Left: total H -exp calls for the 5-, 6-, and 8-factor retractions under fixed step size $t_k = 1/L_{\text{Rie}}$ and exact line search (els). The fitted slopes $s \approx \text{const}$, shown in the legend, confirm the linear dependence $T = \mathcal{O}(\sqrt{N})$. Right: zoom on the exact line search, highlighting that the 6- and 8-factor retractions, despite requiring more H -exp evaluations per iteration, achieve fewer iterations overall and hence a smaller total number of H -exp calls than the 5-factor retraction.

exact line search (els), which requires solving a one-dimensional subproblem to determine the optimal step, i.e.,

$$t_k := \arg \max_{t \geq 0} f(\text{R}_{U_k}(t \text{grad } f(U_k))).$$

Note that, thanks to the classical simulability stated in Theorem 3.6, this line search computation can be carried out efficiently on a classical computer. Recall the explicit process $F(x_k, y_k, q_k; t_k) = (x_{k+1}, y_{k+1}, q_{k+1})$ described in Eq. (25). For fixed values of (x_k, y_k, q_k) , we employ a differential evolution solver to find t_k that maximizes the resulting value of q_{k+1} , and then return the corresponding updated gradient coordinates (x_{k+1}, y_{k+1}) . The exact line search strategy does not require evaluating the Lipschitz constant L_{Rie} . Thus, it can be conveniently applied to any of the three Grover-compatible retractions introduced in Proposition 3.5: the 5-factor, 6-factor, and 8-factor retractions.

Fig. 4 shows that, in all cases, the total number of H -exp (namely $e^{i\theta H}$) calls, equal to the iteration count T multiplied by 2, 3, or 4 respectively, exhibits a linear dependence on \sqrt{N} . The slopes s in the legends quantify this linear scaling. Fig. 4 (left) demonstrates that exact line search significantly improves efficiency, reducing the constant factor hidden in the complexity $T = \mathcal{O}(\sqrt{N})$, even though its theoretical analysis is more involved than that of the fixed $1/L_{\text{Rie}}$ strategy. Fig. 4 (right) zooms in on the three retractions under exact line search. Interestingly, although the 6-factor and 8-factor retractions require more than two H -exp calls per iteration, they achieve fewer iterations overall, and thus yield a smaller total number of H -exp calls than the 5-factor retraction.

Scaling with accuracy Finally, we evaluate how the iteration complexity scales with the target accuracy ε . We fix $n = 15$ qubits and vary ε from 10^{-2} to 10^{-12} in powers of 10. We continue to use the same combination of retractions and step-size strategies as in the previous experiments. Fig. 5 shows that, for all methods, the total number of applications of the H -exp operator grows linearly with $\log_{10}(1/\varepsilon)$, in agreement with the theoretical bound. Over the

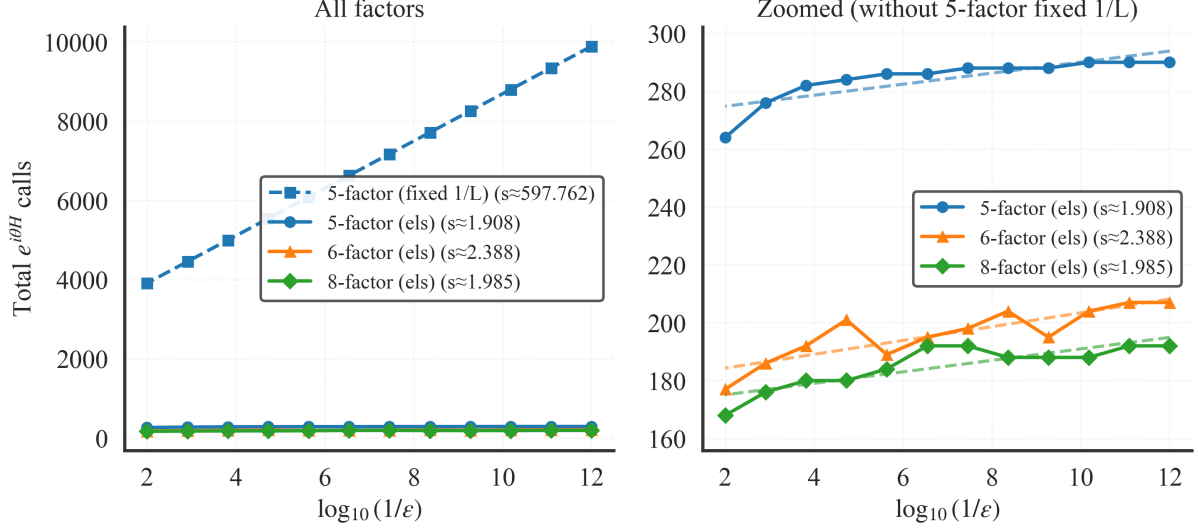


Figure 5: Scaling of the total number of H -exp calls with the target accuracy ε for different Grover-compatible retractions and step size strategies at fixed problem size $N = 2^{15}$. Left: total H -exp calls for the 5-factor retraction with fixed step size $t_k = 1/L_{\text{Rie}}$ and for the 5-, 6-, and 8-factor retractions under exact line search (els), plotted against $\log_{10}(1/\varepsilon)$. The fitted slopes $s \approx \text{const}$, shown in the legend, quantify the effective dependence on $\log_{10}(1/\varepsilon)$. Right: zoom on the three exact line search schemes, together with their fitted lines. The iteration count T almost grows linearly with $\log_{10}(1/\varepsilon)$.

range $\varepsilon \in [10^{-2}, 10^{-12}]$, the exact line search variants exhibit only a very mild increase (5-factor (els): $261 \rightarrow 290$ calls; 6-factor (els): $178 \rightarrow 210$; 8-factor (els): $162 \rightarrow 192$), whereas the fixed-step 5-factor retraction shows a much steeper growth (from 3942 to 9888 calls). This indicates that, even at high accuracy, employing exact line search can substantially improve efficiency. Taken together, Figs. 4 and 5 verify the complexity $\mathcal{O}(\sqrt{N} \log(1/\varepsilon))$ stated in Theorem 4.6, and indicate that this bound is tight in practice.

6 Conclusions

This work offers a new perspective on Grover’s search algorithm from the manifold optimization. Our key contribution is the Grover-compatible retraction, a physically implementable class of retractions. We further show that the optimization dynamics remain confined to a two-dimensional invariant subspace, rendering the algorithm classically simulatable. Using standard nonconvex optimization analysis, our approach recovers the optimal $\mathcal{O}(\sqrt{N})$ quadratic speedup, providing an optimization-theoretic explanation for this quantum advantage.

From an optimization perspective, our Grover-compatible RGA method maps each mathematical iteration directly to a quantum circuit: each update simply appends gates whose generators come from the current Riemannian gradient and whose rotation angle is the step size. This enables optimization theory to move beyond the classical setting and directly inform quantum circuit design on current hardware. This viewpoint suggests several directions for future research:

- A systematic analysis of the optimality of different retractions. As observed in our numerical experiments, the specific choice of retraction directly impacts the pullback’s Lipschitz constant, L_{Rie} . This constant governs the theoretical step size and the resulting complexity upper bound. An optimal retraction would be one that minimizes this Lipschitz constant, thereby yielding the sharpest possible bound and the fastest guaranteed convergence.

- The extension of this framework to other, more advanced optimization methods. While we focused on RGA with a fixed step size (which requires knowledge of L_{Rie}), this perspective opens the door to applying more sophisticated optimization techniques. For instance, adaptive step size rules, such as the Barzilai-Borwein (BB) method [20, 29]. Furthermore, exploring second-order methods, like a Riemannian Newton’s algorithm, is a compelling direction.

Some of the proof strategies in this paper were interactively explored with the assistance of the large language models, and all proofs as presented here were subsequently derived, checked, and written by the authors. A detailed methodological account of this human–AI collaboration, including the interaction protocol and verification procedures, is given in companion paper [33].

References

- [1] Traian Abrudan, Jan Eriksson, and Visa Koivunen. Efficient Riemannian algorithms for optimization under unitary matrix constraint. In *2008 IEEE International Conference on Acoustics, Speech and Signal Processing*, pages 2353–2356. IEEE, 2008.
- [2] P-A Absil, Robert Mahony, and Rodolphe Sepulchre. *Optimization Algorithms on Matrix Manifolds*. Princeton University Press, 2008.
- [3] P-A Absil and Jérôme Malick. Projection-like retractions on matrix manifolds. *SIAM Journal on Optimization*, 22(1):135–158, 2012.
- [4] Giovanni Acampora, Roberto Schiattarella, and Autilia Vitiello. Using quantum amplitude amplification in genetic algorithms. *Expert Systems with Applications*, 209:118203, 2022.
- [5] Roy L Adler, Jean-Pierre Dedieu, Joseph Y Margulies, Marco Martens, and Mike Shub. Newton’s method on Riemannian manifolds and a geometric model for the human spine. *IMA Journal of Numerical Analysis*, 22(3):359–390, 2002.
- [6] Andris Ambainis. Variable time amplitude amplification and quantum algorithms for linear algebra problems. In *STACS’12 (29th Symposium on Theoretical Aspects of Computer Science)*, volume 14, pages 636–647. LIPIcs, 2012.
- [7] William P Baritompa, David W Bulger, and Graham R Wood. Grover’s quantum algorithm applied to global optimization. *SIAM Journal on Optimization*, 15(4):1170–1184, 2005.
- [8] Robert Beals, Harry Buhrman, Richard Cleve, Michele Mosca, and Ronald De Wolf. Quantum lower bounds by polynomials. *Journal of the ACM (JACM)*, 48(4):778–797, 2001.
- [9] Charles H Bennett, Ethan Bernstein, Gilles Brassard, and Umesh Vazirani. Strengths and weaknesses of quantum computing. *SIAM Journal on Computing*, 26(5):1510–1523, 1997.
- [10] Daniel J Bernstein. Post-quantum cryptography. In *Encyclopedia of Cryptography, Security and Privacy*, pages 1846–1847. Springer, 2025.
- [11] Jacob Biamonte, Peter Wittek, Nicola Pancotti, Patrick Rebentrost, Nathan Wiebe, and Seth Lloyd. Quantum machine learning. *Nature*, 549(7671):195–202, 2017.
- [12] Nicolas Boumal. *An Introduction to Optimization on Smooth Manifolds*. Cambridge University Press, 2023.
- [13] Nicolas Boumal, Pierre-Antoine Absil, and Coralia Cartis. Global rates of convergence for nonconvex optimization on manifolds. *IMA Journal of Numerical Analysis*, 39(1):1–33, 2019.

- [14] Gilles Brassard. Searching a quantum phone book. *Science*, 275(5300):627–628, 1997.
- [15] Gilles Brassard, Peter Hoyer, Michele Mosca, and Alain Tapp. Quantum amplitude amplification and estimation. *arXiv preprint quant-ph/0005055*, 2000.
- [16] Carlo Cafaro and Stefano Mancini. On Grover’s search algorithm from a quantum information geometry viewpoint. *Physica A: Statistical Mechanics and its Applications*, 391(4):1610–1625, 2012.
- [17] Daoyi Dong, Chunlin Chen, Hanxiong Li, and Tzyh-Jong Tarn. Quantum reinforcement learning. *IEEE Transactions on Systems, Man, and Cybernetics, Part B (Cybernetics)*, 38(5):1207–1220, 2008.
- [18] Yuxuan Du, Min-Hsiu Hsieh, Tongliang Liu, and Dacheng Tao. A Grover-search based quantum learning scheme for classification. *New Journal of Physics*, 23(2):023020, 2021.
- [19] Christoph Durr and Peter Hoyer. A quantum algorithm for finding the minimum. *arXiv preprint quant-ph/9607014*, 1996.
- [20] Roger Fletcher. On the Barzilai-Borwein method. In *Optimization and control with applications*, pages 235–256. Springer, 2005.
- [21] Austin Gilliam, Stefan Woerner, and Constantin Goniculea. Grover adaptive search for constrained polynomial binary optimization. *Quantum*, 5:428, 2021.
- [22] András Gilyén, Yuan Su, Guang Hao Low, and Nathan Wiebe. Quantum singular value transformation and beyond: exponential improvements for quantum matrix arithmetics. In *Proceedings of the 51st Annual ACM SIGACT Symposium on Theory of Computing*, pages 193–204, 2019.
- [23] Markus Grassl, Brandon Langenberg, Martin Roetteler, and Rainer Steinwandt. Applying Grover’s algorithm to AES: quantum resource estimates. In *International Workshop on Post-Quantum Cryptography*, pages 29–43. Springer, 2016.
- [24] Lov K Grover. A fast quantum mechanical algorithm for database search. In *Proceedings of the twenty-eighth annual ACM symposium on Theory of computing*, pages 212–219, 1996.
- [25] Lov K Grover. Fixed-point quantum search. *Physical Review Letters*, 95(15):150501, 2005.
- [26] Brian C. Hall. *Lie Groups, Lie Algebras, and Representations: An Elementary Introduction*, volume 222 of *Graduate Texts in Mathematics*. Springer International Publishing Switzerland, 2 edition, 2015.
- [27] Ming-Chien Hsu, En-Jui Kuo, Wei-Hsuan Yu, Jian-Feng Cai, and Min-Hsiu Hsieh. Quantum state tomography via nonconvex Riemannian gradient descent. *Physical Review Letters*, 132(24):240804, 2024.
- [28] Jiang Hu, Xin Liu, Zai-Wen Wen, and Ya-Xiang Yuan. A brief introduction to manifold optimization. *Journal of the Operations Research Society of China*, 8(2):199–248, 2020.
- [29] Bruno Iannazzo and Margherita Porcelli. The Riemannian Barzilai-Borwein method with nonmonotone line search and the matrix geometric mean computation. *IMA Journal of Numerical Analysis*, 38(1):495–517, 2018.
- [30] Hamed Karimi, Julie Nutini, and Mark Schmidt. Linear convergence of gradient and proximal-gradient methods under the Polyak-Łojasiewicz condition. In *Joint European conference on machine learning and knowledge discovery in databases*, pages 795–811. Springer, 2016.

- [31] Phillip Kaye, Raymond Laflamme, and Michele Mosca. *An Introduction to Quantum Computing*. Oxford University Press., 2006.
- [32] Donald Ervin Knuth. *The Art of Computer Programming*, volume 3. Pearson Education, 1997.
- [33] Chenyi Li, Zhijian Lai, Dong An, Jiang Hu, and Zaiwen Wen. Advancing mathematical research via human–AI interactive theorem proving. *preprint*, 2025.
- [34] Ze-Tong Li, Xin-Lin He, Cong-Cong Zheng, Yu-Qian Dong, Tian Luan, Xu-Tao Yu, and Zai-Chen Zhang. Quantum comb tomography via learning isometries on Stiefel manifold. *Physical Review Letters*, 134(1):010803, 2025.
- [35] Stanislaw Lojasiewicz. A topological property of real analytic subsets. *Coll. du CNRS, Les équations aux dérivées partielles*, 117(87-89):2, 1963.
- [36] Ilia Luchnikov, Alexander Ryzhov, Sergey Filippov, and Henmi Ouerdane. QGOpt: Riemannian optimization for quantum technologies. *Scipost physics*, 10(3):079, 2021.
- [37] Christopher D Manning. *Introduction to Information Retrieval*. Cambridge University Press, 2008.
- [38] John M Martyn, Zane M Rossi, Andrew K Tan, and Isaac L Chuang. Grand unification of quantum algorithms. *PRX Quantum*, 2(4):040203, 2021.
- [39] Akimasa Miyake and Miki Wadati. Geometric strategy for the optimal quantum search. *Physical Review A*, 64(4):042317, 2001.
- [40] Yurii Nesterov. *Introductory Lectures on Convex Optimization: A Basic Course*, volume 87 of *Applied Optimization*. Springer US, Boston, MA, 2004.
- [41] Michael A Nielsen and Isaac L Chuang. *Quantum Computation and Quantum Information*. Cambridge University Press, 2010.
- [42] Jorge Nocedal and Stephen J Wright. *Numerical Optimization*. Springer, 2006.
- [43] Boris Teodorovich Polyak. Gradient methods for minimizing functionals. *Zhurnal Vychislitel’noi Matematiki i Matematicheskoi Fiziki*, 3(4):643–653, 1963.
- [44] Marcos Raydan. On the Barzilai and Borwein choice of steplength for the gradient method. *IMA Journal of Numerical Analysis*, 13(3):321–326, 1993.
- [45] Quentin Rebjock and Nicolas Boumal. Fast convergence to non-isolated minima: four equivalent conditions for c_2 functions. *Mathematical Programming*, pages 1–49, 2024.
- [46] Hiroyuki Sato and Kensuke Aihara. Cholesky QR-based retraction on the generalized Stiefel manifold. *Computational Optimization and Applications*, 72(2):293–308, 2019.
- [47] Yohichi Suzuki, Shumpei Uno, Rudy Raymond, Tomoki Tanaka, Tamiya Onodera, and Naoki Yamamoto. Amplitude estimation without phase estimation. *Quantum Information Processing*, 19(2):75, 2020.
- [48] Yudai Suzuki, Marek Gluza, Jeongrak Son, Bi Hong Tiang, Nelly HY Ng, and Zoë Holmes. Grover’s algorithm is an approximation of imaginary-time evolution. *arXiv preprint*, 2025. arXiv:2507.15065.
- [49] Mario Szegedy. Quantum speed-up of Markov chain based algorithms. In *45th Annual IEEE Symposium on Foundations of Computer Science*, pages 32–41. IEEE, 2004.

- [50] Zaiwen Wen and Wotao Yin. A feasible method for optimization with orthogonality constraints. *Mathematical Programming*, 142(1):397–434, 2013.
- [51] Roeland Wiersema and Nathan Killoran. Optimizing quantum circuits with Riemannian gradient flow. *Physical Review A*, 107(6):062421, 2023.
- [52] Theodore J Yoder, Guang Hao Low, and Isaac L Chuang. Fixed-point quantum search with an optimal number of queries. *Physical Review Letters*, 113(21):210501, 2014.
- [53] Christof Zalka. Grover’s quantum searching algorithm is optimal. *Physical Review A*, 60(4):2746, 1999.